Mon. Not. R. astr. Soc. (1971) **153**, 337–382.

CHARACTERISTICS OF THE RADIO PULSES FROM THE PULSARS

A. G. Lyne, F. G. Smith and D. A. Graham

(Received 1971 March 13)

SUMMARY

The shape and structure of radio pulses from the majority of the pulsars have been studied at frequencies of 151, 240, 408 and 610 MHz, using polarimeter receivers. Individual pulses from the stronger pulsars have been recorded photographically. The integrated pulse profiles have been obtained from on-line integration of the four Stokes parameters. Many of the results are presented graphically; the main characteristics are collected in a table.

A discussion of the pulse widths and the change of polarization angle within the pulses supports the view that the integrated pulse profile represents a longitude distribution of emission, while the individual pulses represent individual beams of radiation. The changes of position angle within the profile suggest that the magnetic field has a simple configuration in the emitting region, and that it may resemble the equatorial part of a dipole field.

New measurements of the rotation measures of five pulsars are presented together with a compilation of nine previous results. Some new measurements of period and position are also presented.

1. INTRODUCTION

The radio pulses from the pulsars exhibit many complex characteristics, which vary both between successive pulses and from one pulsar to another. It has been found that the sum of many pulses, forming an integrated profile, is characteristic of an individual pulsar: the duration and shape of this profile has been used in constructing models of the emitting regions of pulsars. The individual pulses are, however, also found to have a characteristic width for each pulsar, and this width has been interpreted as the width of a rotating beam of emission. The individual pulses are highly polarized, and their state of polarization varies through the pulse. When many pulses are added to produce an integrated profile, the integrated polarization is often much smaller, since there is a variability of polarization both within the pulse and from pulse to pulse.

This paper describes observations both of the individual pulses and of the integrated profiles. Individual pulses were recorded photographically, using a polarimeter receiver which measured the four Stokes parameters I, V, Q, U simultaneously for each pulse. (These parameters may loosely be described as the total intensity, the circularly polarized component, and the two orthogonal components of the linear polarization—see for example Born & Wolf 1965). The four receiver outputs were also integrated digitally in an on-line computer to give the integrated profiles.

The most comprehensive set of observations was made at 408 MHz, but many pulsars have also been studied at 151, 240 and 610 MHz. We are therefore able to report on the frequency dependence of several characteristics over a 4 : 1 frequency range.

2. OBSERVING TECHNIQUES

2.1 *Antenna systems*

Polarimeter feeds were installed at the focus of the Mk I 250-ft radio telescope, usually for a single frequency; for some comparative observations a multiple feed was used which operated simultaneously at 151, 240 and 408 MHz. The single frequency feeds consisted of orthogonal dipoles with dipole reflectors. The combined feed consisted of orthogonal dipoles for 408 MHz, surrounded by two squares of dipoles each one half wavelength on the side for the two lower frequencies, where each linear polarization was represented by a pair of dipoles connected in parallel. A ground plane reflector was used for the combined feed. For each frequency the signals from the two plane polarized feeds were connected through hybrid circuits to the inputs of two receivers. In this way the signal voltages X, Y in the orthogonal dipoles were combined in quadrature as $(X+iY)$, $(iX+Y)$ in the receiver inputs, so that a circularly polarized signal appeared in one receiver only, while a linearly polarized signal appeared in both with a phase difference depending on its position angle.

Calibration signals could be radiated into the polarimeter feed from dipoles mounted 3 m in front of the feed, where the four support legs of the focus cabin join at the top of the central tower of the reflector. These dipoles were fed by a noise generator which could be pulsed so as to simulate a linearly polarized pulsar signal.

The alignment of the dipoles, the adjustment of cable lengths, and the match of impedance to the hybrid circuits, were all sufficiently accurate that cross-coupling between different modes of polarization was less than 1 per cent. There remain the effects of imperfections in the reflector and the feed supports, and in the receiving apparatus: these were investigated in calibrations of the complete system, as described in Section 2.4.

2.2 *Receiver systems*

The two receivers consisted of low-noise amplifiers (varactor diode parametric amplifiers at 610 and 408 MHz, F.E.T. amplifiers at 240 and 151 MHz), followed by mixers fed from a common local oscillator, and I.F. amplifiers at 30 MHz. Signals at this frequency were fed from the telescope to the observing room, where the detectors were located. The RF and IF amplifiers had comparatively wide bandwidths, and the frequency characteristics of the systems were determined completely by matched pairs of filters, in which the relative phase transmission characteristics were practically independent of frequency. Bandwidths of 100 kHz, 330 kHz, or 1 MHz were used for most observations.

The total intensity (I) was obtained from the sum of the detected outputs of the two channels, and the circularly polarized component (V) from the difference. The plane polarized components (Q, U) were obtained by multiplication, giving in-phase and quadrature components. This was achieved by combining the two signals in further hybrid networks, and using matched pairs of detectors. A linearly polarized signal with power p, and position angle ϕ relative to the position of the calibration dipole then gave outputs proportional to $p \cos 2\phi$ and $p \sin 2\phi$.

The unwanted cross couplings in the detector system were all less than 3 per cent for signals up to four times the system noise level. (Some observations reported in this paper were, however, made at earlier observing sessions when the accuracy was rather worse, especially in the measurement of V; a special note is made of any results affected by this.)

2.3 *Recording systems*

The detector outputs were amplified and displayed on a four-trace oscilloscope which was triggered synchronously with the pulsar.

The outputs were also connected to voltage-to-frequency converters which fed a pulse averaging system. This was an adaption of the digital correlator described by Davies, R. D. *et al.* (1969). Signal sampling was achieved in the multiplier circuits of this apparatus by sending a logical '1' down the shift register once per pulsar period; the multiplication products were then stored in the binary counters. The result of this operation was that each counter contained a number proportional to the signal voltage at a particular phase of the pulsar period. The phase interval between adjacent counters was simply determined by the rate at which the contents of the shift register were shifted.

The digital correlator contains 256 channels, all of which could be used to provide high resolution on an integrated pulse profile. For most of our observations, however, they were divided into four independent sections of 64 channels, each section integrating one of the four Stokes parameters.

The integrated data so obtained was read into the on-line ARGUS 400 computer which presented the data on a curve plotter and stored the data on paper tape for later analysis.

The computer program which controlled the observations contained an ephemeris to correct pulsar periods for the motion of the observatory in the Solar System, so that integrations could be continued without any adjustment for some hours, even in the case of the fastest pulsar PSR 0531+21.

The material for our analysis consists mainly of photographed sequences of pulses, observed as individuals on the oscilloscope, and the recordings of integrated Stokes parameters from the on-line computer. The computer also controlled the pulsed noise source which provided a calibration of the position angle, the sensitivity of the system, and the cross-coupling between linear and circular polarization. These calibrations were therefore available in the integrated data.

2.4 *System accuracy*

Although the separate parts of the polarimeter receiving system were set up to sufficient accuracy, it remained to check the complete system, including the effects of the feed support. This was achieved by observing unpolarized discrete sources such as Taurus A, together with the linearly polarized calibration signal. The feed could be rotated, and it was found that asymmetries in the feed supports and the reflector surface could produce cross-couplings amounting to 6 per cent in the worst case. At the best settings of the feed system, the cross-couplings are all less than 3 per cent.

The two separate sources of spurious linear polarization, from the telescope and from the correlation receiver, may combine vectorially to produce an error up to 6 per cent. For most observations, however, this error was reduced to 3 per cent either by adjustment or by using the calibrations to produce suitable correction factors. The correct measurement of circular polarization depends on the balance between the sensitivities of two receiver channels and errors of up to 10 per cent may occur. Again, by adjustment or through calibration, this error could be reduced to below 5 per cent.

Values of percentage polarizations depend on the relative sensitivity of the output channels; errors here were usually less than 10 per cent of the values quoted in our results. The final accuracy of most results was set by the available signal to noise ratio, and special efforts to improve calibration accuracies were only made for a few pulsars.

2.5 *The effect of dispersion*

The dispersive propagation in the ionized interstellar gas may delay the pulses by appreciably different times across the receiver bandwidth, so that the pulse is artificially lengthened. (For very distant pulsars there is also a lengthening due to multi-path propagation which occurs even with a very narrow bandwidth (Davies, J. G., Large & Pickwick 1970); we note separately the few situations where this may affect our observations.) The dispersion delay at frequency ν (MHz) of a pulse with dispersion measure D (in pc cm^{-3}) is $4 \cdot 1 \times 10^6 \, D\nu^{-2}$ ms; differentiation gives the difference in delay across a receiver bandwidth B (MHz) at the four receiver frequencies as kBD ms, where k has the following values: 2·5 at 151 MHz, 0·63 at 240 MHz, 0·13 at 408 MHz, and 0·038 at 610 MHz. Most of the known pulsars have dispersion measures lying in the range 10–100. Receiver bandwidths of 0·1 or 0·3 MHz were therefore adequate for resolution down to about 1 ms at 610 and 408 MHz, but the effect of dispersion was often serious at the lower frequencies.

3. STUDIES OF PSR 0329+54

A comprehensive study of this pulsar has been made at all four observing frequencies. The results illustrate well the relation between individual pulses and the integrated profile, and we present them separately so as to bring out some points which seem to apply generally to all pulsars.

3.2 *The identification of individual pulses*

Fig. 1 shows a tracing of a photographic recording of a sequence of pulses from PSR 0329+54. The oscilloscope time base is triggered accurately at the mean period, but the individual pulses occur at different points in the trace, which covers a time of 40 ms. We refer to this as a variation in 'pulse phase'. The shapes of the intensities (I) of these pulses are not limited by dispersion or by any receiver time constant; nevertheless they show generally the same shape and width at all pulse phases. Fig. 1 also shows the central part of the integrated profile for pulses from this pulsar at the same radio frequency. There are also two outer parts in the profile of PSR 0329+54, usually known as the 'outriders'; these are shown in later figures. One of the oscilloscope traces shows an isolated pulse occurring at the time of the 'shoulder' on the leading edge of the profile; again the pulse has the same typical shape and width.

Sequential pulses from some pulsars appear with a steady drift in pulse phase, usually to an earlier phase (Drake & Craft 1968). The integrated profile then appears to be a modulation envelope, which determines the relative strength of the pulse at different phases. For other pulsars, particularly those with complex integrated profiles, it seems that the appearance of pulses in different parts of the

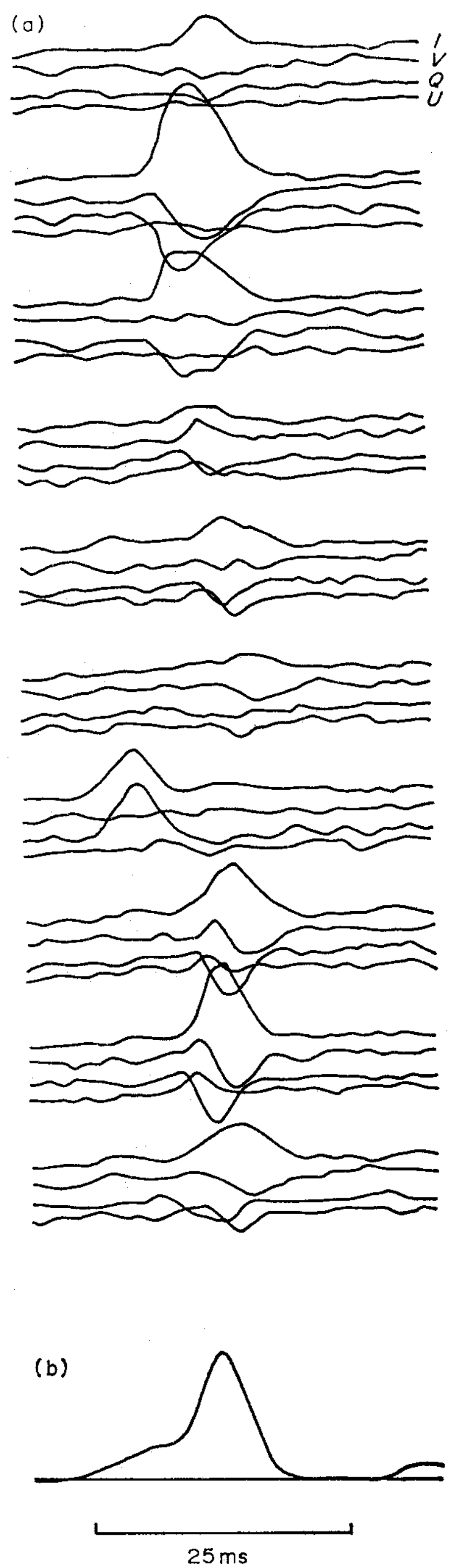

FIG. 1. (*a*) *A sequence of pulses from PSR 0329+54, recorded with a polarimeter at 408 MHz. The four traces show the Stokes parameters I, V, Q, U.* (*b*) *The integrated profile obtained by addition of the intensity I of several hundred pulses.*

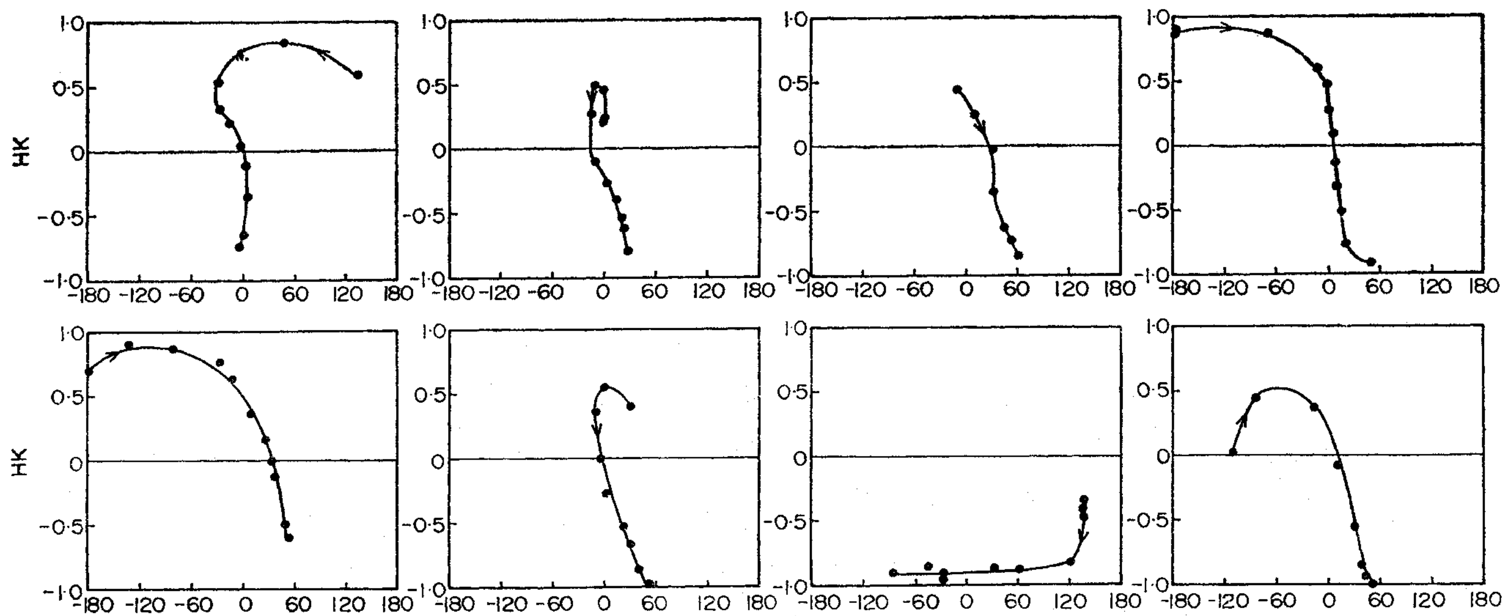

FIG. 2. *The varying elliptical polarization of individual pulses from PSR 0329+54. The Stokes parameter V is plotted against 2ϕ, twice the position angle of polarization. The points on the curve are at uniform time intervals of 1 ms.*

profile is not obviously correlated, so that the integrated profile appears to represent the probability that a pulse will appear at any pulse phase.

3.3 *Polarization of individual pulses*

The individual pulses are very highly polarized (Clark & Smith 1968). Whenever a symmetrical isolated pulse appears, the polarization is approximately 100 per cent, and seldom less than 70 per cent throughout the pulse. The polarization is generally elliptical. In Fig. 2 the polarization ellipse throughout several pulses is described by a plot of V against 2ϕ. The amplitude of the pulse does not appear in these plots; V has been normalized so that a completely circular polarization would be plotted as $V = \pm 1$ according to the hand.

The polarization ellipse changes smoothly during a single pulse. The position angle may change by any amount up to 90°, but no more. The value of V may change by any amount, including almost the full range $+1 \rightarrow -1$; but the direction of change can reverse only once during the pulse. These changes correspond to a traversal of the Poincaré sphere (Born & Wolf, *loc cit*, p. 31) along an arc of a great circle which extends more than 180° but which can run at any orientation. (Fig. 2 is in fact a Mercator projection of the Poincaré sphere.)

3.4 *Frequency dependence of the pulse width and polarization*

The highly organized and simple behaviour of the polarization within individual pulses suggests strongly that these represent elemental beams of radiation sweeping past the observer as the pulsar rotates, in the manner of a rotating beamed antenna. It is therefore very remarkable that the width and polarization characteristics are not markedly dependent on frequency, as noted by Smith (1969, 1970a). At 240, 408 and 610 MHz we find that the characteristic width of pulses from PSR 0329+54 is within the range $4 \cdot 5 \pm 0 \cdot 5$ ms. At 151 MHz the measured width is increased by dispersion, but there still appears to be no change in the intrinsic width.

The plane of polarization does, of course, depend on frequency on account of Faraday rotation in the interstellar medium. The circular component is, however, unaffected, and it is found that the parameter V behaves similarly in pulses at all four frequencies. Some individual pulses have been recorded both at 240 MHz and 408 MHz, when the width and reversing pattern of V were found to be identical (Smith 1970b).

The rather small amount of evidence on pulses from other pulsars supports the conclusion that the pulse width and the polarization do not depend markedly on frequency.

3.5 *The relation between individual pulses and integrated profiles*

The variability of the individual pulses in pulse phase and in polarization contrasts strongly with the constancy of the integrated profile. The width of the profile evidently represents a limited range of pulse phase within which the pulse can occur; equally the existence of finite integrated polarization shows that the variable polarization of the individual pulses is not completely random. Figs 1 and 2 show that the polarization does vary through the individual pulses in a variety of ways. There seems to be no ordering of this variation other than that which appears in the integrated polarization.

The circular component of polarization tends to reverse within individual pulses, and the pulse phase of this reversal is variable. This variation appears to be responsible for the large reduction of the circular component on integration There is, nevertheless, a definite value for the integrated V, amounting to 10 per cent and reversing during the profile (Graham 1971).

We conclude that for each part of the integrated profile there is a preferred state of polarization; individual pulses differ from this state in a random way. Again illustrating states of polarization as points on a Poincaré sphere, it seems that a single typical point can be assigned to each pulse phase, but that the polarization at that phase within any individual pulse can be represented by a point lying within a defined area around that typical point.

3.6 *The integrated profile as a function of frequency*

Fig. 3 shows the integrated profiles for PSR 0329+54 at 240, 408 and 610 MHz, including the linear polarization in the form of an intensity P and a position angle ϕ. The intensity P is obtained from the averaged values of the Stokes parameters Q and U, combined to provide $P = (Q^2+U^2)^{1/2}$ and $\phi = \frac{1}{2}\tan^{-1} U/Q$. The angle ϕ is presented only where the r.m.s. error is less than 20°. Adjacent data points are completely independent.

The three profiles are generally very similar. Two differences in detail appear in the position of the leading ' outrider ' component, and in the intensity between the main component and the trailing outrider. The time interval between the leading outrider and the main component is approximately equal to

$$28\left(\frac{\nu}{300}\right)^{-0.17} \text{ms},$$

where ν is the frequency in MHz. Similar variations in spacing have been found for PSR 1133+16 (Craft & Comella 1968) and other pulsars; details will be found in Section 5 of this paper.

The position angle ϕ varies in a similar way through the profile at all three frequencies. (The absolute values of ϕ have not been calculated: they depend on a precise knowledge of the Faraday rotation in the ionosphere and in interstellar space.) It is notable that the variation is continuous through the whole profile, including the bridge between the main and trailing outrider components. Further, although the evidence is less clear, it seems that ϕ varies smoothly through the time of the early outrider, and that the variation of ϕ is roughly the same at all three frequencies despite the different positions of the early outrider.

The profiles of integrated intensity shown in Fig. 3 represent the normal mode of PSR 0329+54. Lyne (1971b) has found that for periods of about half an hour at intervals of a few hours a different profile occurs, with the leading outrider doubled and the trailing outrider halved in intensity. The variation of ϕ through the profile is unchanged at these times.

4. INDIVIDUAL PULSE SHAPES AND POLARIZATIONS

The detailed study of PSR 0329+54 cannot be extended to many pulsars, since it requires a good signal-to-noise ratio for individual pulses. Wherever it has been possible to photograph individual pulses, it has again been found that these generally are considerably narrower than the integrated profile; they are also highly polarized, and they have a width which is typical for each pulsar. The details of their occurrence within the profile vary: for example individual

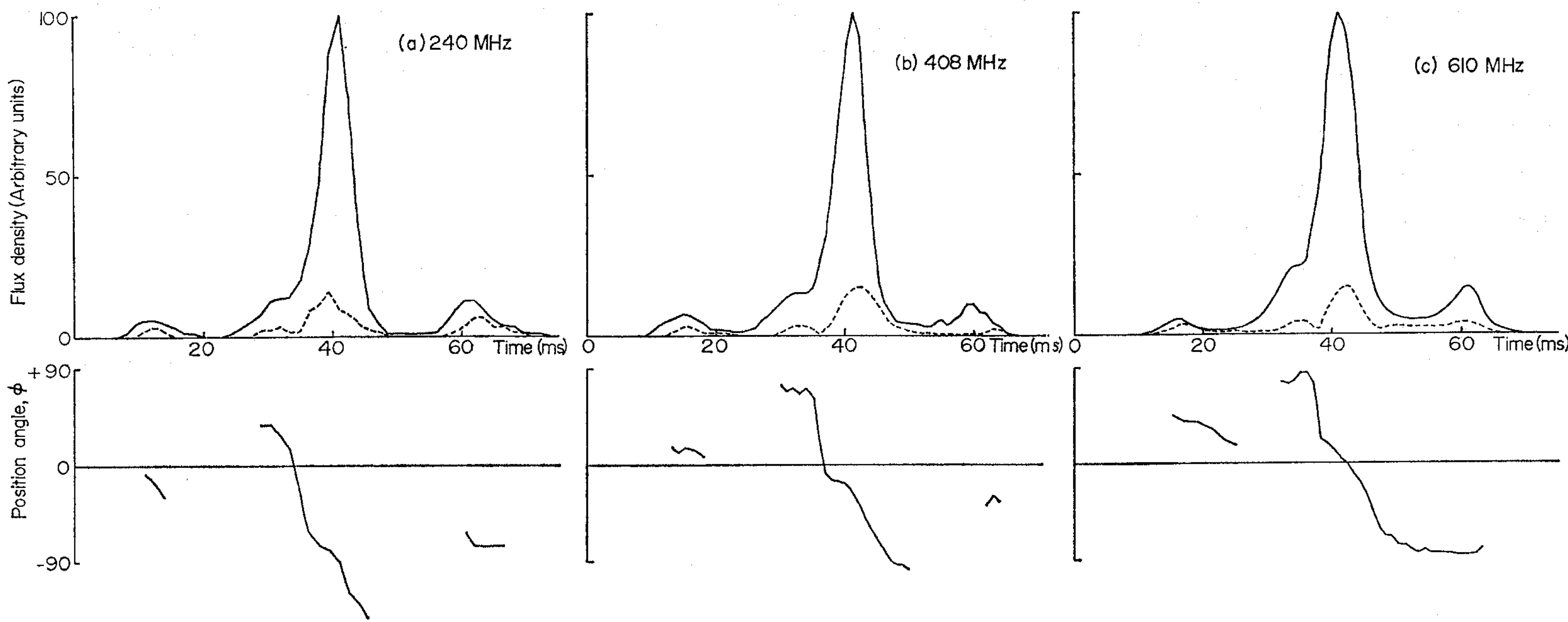

FIG. 3. *Integrated profiles for PSR 0329+54 at 240, 408 and 610 MHz, showing the intensity I, and the linear polarization P with position angle* ϕ.

TABLE I

PSR	Period (s)	Equivalent width integrated (ms)	Equivalent width integrated (° long)	Shape integrated profile	Width individuals (ms)	Width individuals (° long)	Integrated linear polarization, per cent 151	240	408	610	Position angle rotation Angle	(° long)	Phase rate	Freq. MHz	Notes
0031−07	0·943	60	24	Single	~10	~4	—	~20	—	—	−30	40	−0·8	240	Individual width estimated from Sutton *et al.* (1970).
0254−54	0·448	—	—	—	—	—	—	—	—	—	—	—	—	—	—
0329+54	0·715	9·0	4·5	Single with outriders	4·5	2·2	20	20	20	18	−170	8	−21	—	Equivalent width includes outriders. V reaches 10 per cent, reversing $L \rightarrow R$.
0450−17	0·549	27	17	Triple (?)	—	—	—	—	20	—	−55 +40	5 14	−11 +3	—	—
0525+21	3·745	83	8	Double	—	—	—	—	50	60	−25 −5	5 5	−5 −1	610	Step in P.A. between peaks.
0531+21	0·033	1·2	13	Precursor and interpulse	—	—	—	—	—	—	—	—	—	—	Precursor polarized ~80 per cent.
0628−28	1·244	57	17	Single	40	11·5	—	~60	60	80	+110	45	+2·5	610	85 MHz Vitkevich & Shitov (1970b). 150 MHz Schwarz & Morris (1971). 1720 MHz Komesaroff *et al.* (1970). 2650 MHz Morris *et al.* (1970).
0736−40	0·375	18	17·5	Double	—	—	—	—	—	—	—	—	—	—	Equivalent width from Komesaroff *et al.* (1970).
0740−28	0·167	—	—	—	—	—	—	—	—	—	—	—	—	—	Bologna: IAU Circular 2295.
0809+74	1·292	48	13·5	Single	3·5	1·0	20	10	15	—	−10 −5	10 8	−1·0 −0·6	151	Step in P.A. Individual width estimated from Sutton *et al.* (1970) and Cole (1970).
0818−13	1·237	23	6·7	Single	—	—	—	10	25	—	+20 +70	5 1½	+4 +47	—	—

1971MNRAS.153..337L

0823+26	0·531	6·7	4·5	Single	4	2·7	—	30	30	25	+55	7	+8	—	Equivalent width 4·8° at 240 MHz. Equivalent width 3·3° at 610 MHz.
0833−45	0·089	2·1	8·7	Single	—	—	—	—	—	—	−95	19	−5	1720	Equivalent width from Ables *et al.* (1970). Polarization from Komesaroff *et al.* (1970); who give 90 per cent polarization at 635 MHz.
0834+06	1·274	18	5·2	Double	4	1·3	25	22	10	<15	+65 −50 +150	1·5 5·6 6	+43 −9 +25	} 151 408	P.A. rotates ∼+155° in 6° at 408 MHz. *V* (at 240 MHz and at 408 MHz) reaches 15 per cent and reverses.
MP 0835	0·765	—	—	—	—	—	—	—	—	—	—	—	—	—	—
0904+77	1·579	—	—	Single with interpulse	—	—	—	—	—	—	—	—	—	—	Taylor & Huguenin (1969).
MP 0904	0·662	—	—	—	—	—	—	—	—	—	—	—	—	—	—
0943+10	1·098	—	—	—	—	—	—	—	—	—	—	—	—	—	—
0950+08	0·253	10	14	Single with interpulse	1–2	1·5–3	70	50	45	10	−160	85	−1·9	—	P.A. rotation possibly continuous over 210°. 2700 MHz Komesaroff *et al.* (1970).
0959−54	1·437	—	—	—	—	—	—	—	—	—	—	—	—	—	—
1133+16	1·188	18	5·4	Double	3·5	1·0	35	35	30	25	+85	10	+8·5	240	*V* reaches 15 per cent and reverses. 2650 MHz Morris *et al.* (1970).
MP 1154	0·400	—	—	—	—	—	—	—	—	—	—	—	—	—	—
1237+25	1·382	20	5·2	Complex, extending over 17°	6	1·5	35	45	75	∼70	<10	16	<0·7	151	*V* reaches 50 per cent for ∼5 ms near centre of profile.
1240−63	0·388	—	—	—	—	—	—	—	—	—	—	—	—	—	—
MP 1359	0·690	—	—	—	—	—	—	—	—	—	—	—	—	—	—
MP 1426	0·788	—	—	—	—	—	—	—	—	—	—	—	—	—	—
MP 1449	0·180	—	—	—	—	—	—	—	—	—	—	—	—	—	—

TABLE I (*continued*)

PSR	Period (s)	Equivalent width integrated (ms)	Equivalent width integrated (° long)	Shape integrated profile	Width individuals (ms)	Width individuals (° long)	Integrated linear polarization, per cent 151	240	408	610	Position angle rotation Angle	(° long)	Phase rate	Freq. MHz	Notes
1451−68	0·263	12·5	17	Single	—	—	—	—	—	—	—	—	—	—	2650 MHz Morris *et al.* (1970).
1508+55	0·740	13	6·4	Single	—	—	~10	~10	25	45	−200	11	−17·5	—	*V* reaches 25 per cent and reverses.
1530−53	1·369	—	—	—	—	—	—	—	—	—	—	—	—	—	—
1541+09	0·748	44	21	Single	—	—	—	~40	—	—	<20	12	<1·7	240	*V* reaches 25 per cent.
1604−00	0·421	10	9·2	Close double	—	—	—	—	15	—	−110	9·5	−12	—	*V* reaches 15 per cent. Step in P.A.
1642−03	0·388	4·0	3·6	Single	4	3·7	70	30	25	15	+15	3	+5	—	*V* reaches 15 per cent at end of profile.
1706−15	0·654	13	7·0	Single	—	—	—	—	20	—	—	—	—	—	Irregular rotation of P.A.
1727−47	0·830	—	—	—	—	—	—	—	—	—	—	—	—	—	—
1747−46	0·742	—	—	—	—	—	—	—	—	—	—	—	—	—	—
1749−28	0·563	7·0	4·5	—	6	3·8	—	25	20	—	+60	5	+12	2650	2650 MHz Morris *et al.* (1970).
1818−04	0·598	12·5	7·5	Single	—	—	—	—	15	—	—	—	—	—	—
1845−04	0·598	27	16	Single	—	—	—	—	—	—	—	—	—	—	—
1857−25	0·612	35	20	Complex	—	—	—	—	20	—	−10 −200 <10	10 12 12	−1·0 −16 <0·8	—	*V* reaches 30 per cent and reverses during rapid change of P.A.
1858+03	0·655	20	11	Single	—	—	—	—	—	—	—	—	—	—	Equivalent width at 610 MHz. Broadened at lower frequencies by scattering. (DM = 400.)

1911 − 04	0·826	7·3	3·2	Single	—	—	—	—	<7	—	—	—	—	—	—
1919 + 21	1·337	25	6·8	Double	6	1·6	<15	13	12	—	—	—	—	—	P.A. rotation complex.
1929 + 10	0·227	5·7	9·1	Single with interpulse	—	—	—	90	85	80	−35	26	−1·3	—	2650 MHz Morris *et al.* (1970). 2700 MHz Komesaroff *et al.* (1970). 2650 MHz Morris *et al.* (1970).
1933 + 16	0·359	6	6·1	Single	—	—	—	—	15	25	—	—	—	—	Equivalent width at 610 MHz. Broadened at lower frequencies by scattering (DM = 157).
1944 + 17	0·440	23	19	Single	—	—	—	—	20	—	—	—	—	—	—
1946 + 35	0·717	11	5·7	Single	—	—	—	—	30	20	—	—	—	—	—
1953 + 29	0·427	20	17	Single	—	—	—	—	—	—	—	—	—	—	—
2003 + 31	2·11	21	3·6	Single	—	—	—	—	—	—	—	—	—	—	—
2016 + 28	0·558	15	9·6	Single	~5	~3	—	25	35	—	+30	6·5	+4·5	—	—
2020 + 29	0·344	—	—	—	—	—	—	—	—	—	—	—	—	—	Bologna: IAU Circular 2287.
2022 + 51	0·529	18	12	Double	—	—	—	—	60	25	+30	14	+2·2	—	Manchester (1970).
2045 − 16	1·962	41	7·5	Triple extending over 18°	4	0·7	25	40	35	55	0 −125 −15	4 6·5 3·5	0 −28 −6	—	*V* reaches 25 per cent in centre of profile (408 MHz). 2700 MHz Komesaroff *et al.* (1970). 2650 MHz Morris *et al.* (1970).
2113 + 46	1·015	29	10	Single with outriders out to ±40°	—	—	—	—	35	—	+35	1	+35	—	—
2217 + 47	0·538	9	6·0	Single	—	—	—	20	15	60	—	—	—	—	Polarization >70 per cent at 100 MHz (Shitov 1971).
2303 + 30	1·576	35	8	—	—	—	—	—	—	—	—	—	—	—	—
2319 + 60	2·256	140	22	—	—	—	—	—	—	—	—	—	—	—	—

pulses from PSR 1642−03 and PSR 1749−28 are nearly as wide as the profile itself, and the time of occurrence varies only slightly; at the other extreme the pulses from PSR 1133+16 are only about 4 ms wide compared with the double humped integrated profile which covers over 40 ms. In the latter case, as with other pulsars with complex integrated profiles, the pulses seem to arrive independently of one another, although two may happen to arrive together, one in each part of the double profile.

There is in some pulsars a tendency for two or more pulses to appear together, at a fairly well-defined separation. Pulses are often related from one period to the next, appearing with a slow variation of pulse phase. Both phenomena are displayed by PSR 2016+28. Studies of this 'pulse drift' have been made by Drake & Craft (1968), Cole (1970), Sutton *et al.* (1970), Backer (1970a, b) and others whose work is referred to in those papers.

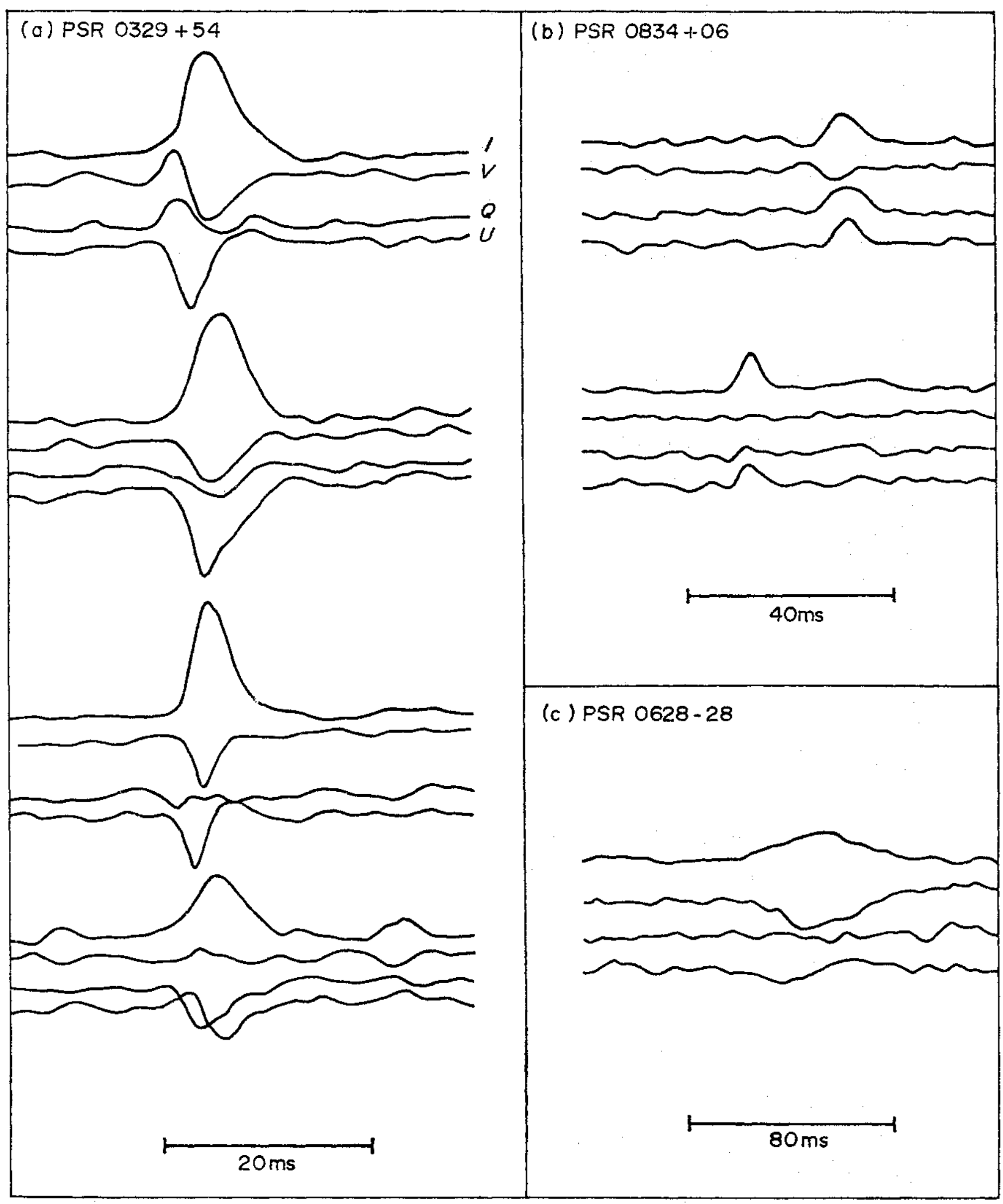

FIG. 4. *Individual pulses from three pulsars, observed at 240 MHz with a polarimeter recording the four Stokes parameters I, V, Q, U. (a) PSR 0329+54. (b) PSR 0834+06. (c) PSR 0628−28.*

We have usually found the definition of a typical single pulse unambiguous; but for PSR 0950+08 the situation appears complex. Here the most frequently occurring component is about 2 ms wide, but there are also many pulses over 5 ms wide inside which the polarization varies only slowly, and remains very high, while the intensity varies in a more complex manner. A similar behaviour can be seen in some pulses from PSR 1133+16.

We have attempted to find for each pulsar a typical pulse, which corresponds to the typical pulse from PSR 0329+54. This is roughly Gaussian in profile, and contains a smoothly varying polarization. The half-width of this pulse is listed in Table I, both in milliseconds and as a range of pulse phase. The following are some detailed notes on individual pulsars.

PSR 0031−07. The work of Sutton *et al.* (1970) shows that individual pulses are not greater than 10 ms wide.

PSR 0531+21. Although highly polarized individual pulses from the Crab Nebula pulsar have been recorded (Graham, Lyne & Smith 1970; Heiles, Campbell & Rankin 1970), it is impossible to resolve the pulse structure with a single receiver channel, on account of the high dispersion. (For example Heiles *et al.* use the comparatively narrow bandwidth of 8·2 kHz at 430 MHz, so as to reduce the effect of dispersion: it follows that any receiver output at their time resolution of 120 μs will be fully modulated in a random manner, so that their records of variations of polarization on their time scale are not meaningful.) It only seems possible to assign an upper limit of about 1 ms on the pulse width. There has been no certain detection of circular polarization.

PSR 0628−28. A single recording on 240 MHz (bandwidth 350 kHz, time constant 3 ms), shows several pulses of which that in Fig. 4 is typical. There is a rapidly changing position angle in this pulse.

These pulses are the longest in relation to the period of any pulsar in which individual pulses have been detected.

PSR 0809+74. Uncertain measurement of only two pulses at 240 MHz, (bandwidth 350 kHz), pulse width ~3 ms, linearly polarized with little swing of position angle.

PSR 0823+26. A recording of *I* only on 408 MHz (bandwidth 300 kHz), shows five simple pulses all ~4 ms width in 2 min. Ekers & Moffet (1969) show a single pulse recorded at 13-cm wavelength which appears to be somewhat narrower, and also suggest that structure as narrow as 0·1 ms can be seen.

PSR 0833−45. Ekers & Moffet (1969) quote time scales from 2 to 0·3 ms or less.

PSR 0834+06. Recordings at 240 MHz (bandwidth 300 kHz) show pulses of which those in Fig. 4 are typical. The pulses show predominantly plane polarization with little swing of position angle. The pulse width corrected for bandwidth (2·5 ms) and time constant (3 ms) is approximately 4 ms.

PSR 0950+08. The pulses are variable and complex. Fig. 5 shows a sequence of pulses at 408 MHz, bandwidth 300 kHz, time constant 0·1 ms. There is no structure finer than about 2 ms in width which is not attributable to random noise. There are some pulses about 2 ms long which are like the typical pulses of other pulsars; other pulses are longer lasting 10 ms or more, but their structure suggests that they are made up of components about 2 ms long. These more complex pulses often appear to be nearly unpolarized, while others may show a consistent plane of polarization for about 5 ms. This behaviour may be explained by the superposition of individual pulses, although it must be remembered that the complex pulses with consistent polarization might equally well represent an intensity modulation acting on a longer basic pulse.

Observations by Ekers & Moffet (1968) at 2295 MHz show structure with a time scale less than 1 ms.

PSR 1133+16. The four pulses shown in Fig. 5 occurred within one minute. The structure seems to be fully resolved, using an effective time constant of 0·5 ms at 408 MHz (bandwidth 330 kHz). Single pulses, about 4 ms wide, are seen to occur either as groups or as simple individuals at times corresponding to the two peaks in the integrated profile. In some complex pulses there are fluctuations which are more marked in intensity than in polarization: these may

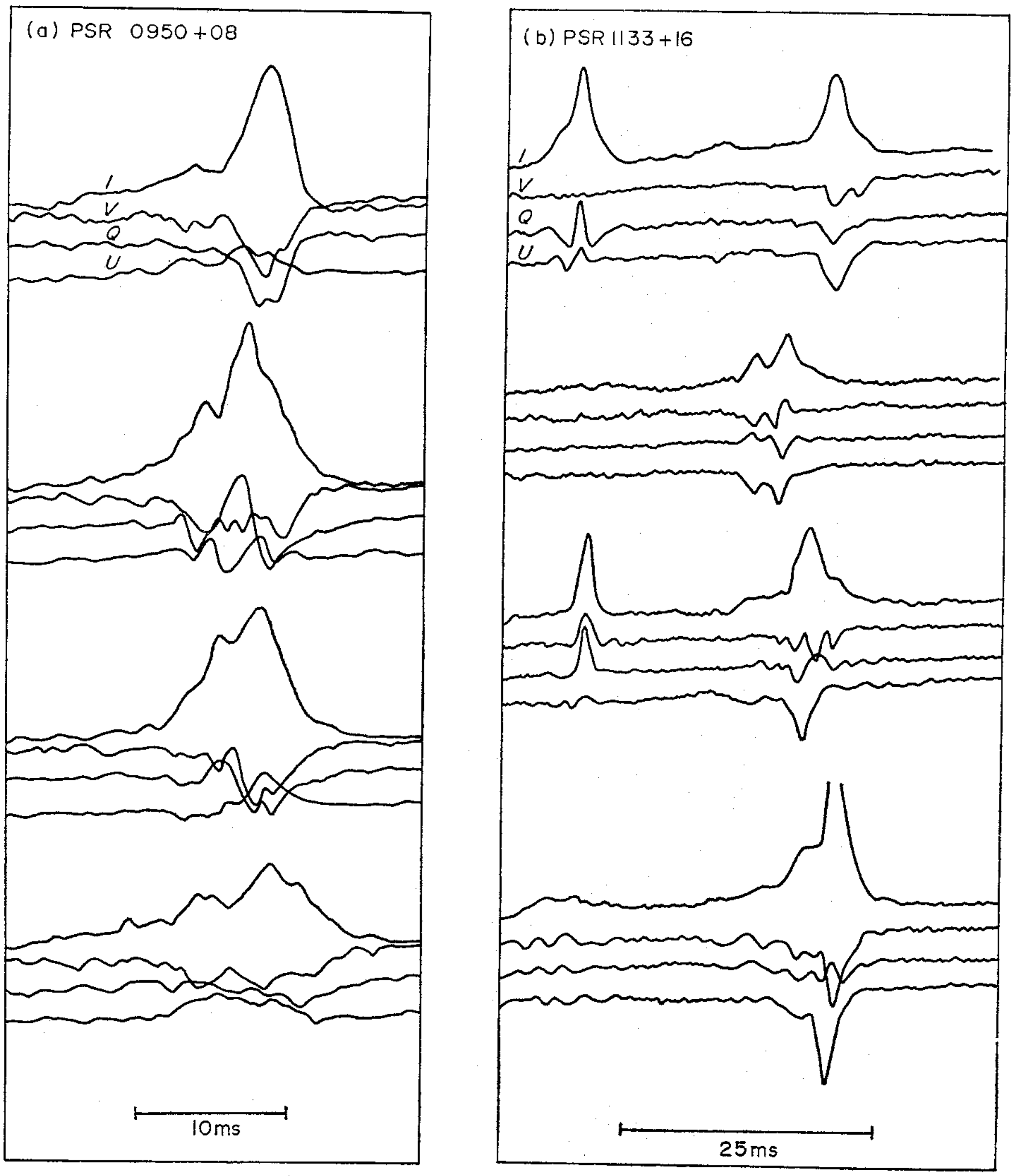

FIG. 5. *Individual pulses from two pulsars: (a) PSR 0950+08, (b) PSR 1133+16, recorded with a polarimeter at 408 MHz. The four traces show the Stokes parameters I, V, Q, U. The pulses from PSR 0950+08 were sequential: those from PSR 1133+16 were recorded within one minute.*

represent an intensity modulation of a broader source, but it remains the simplest interpretation to regard them as the sum of a number of separate individuals, like those which stand out in Fig. 5.

The position angle of polarization in pulses occurring in the earlier component of the integrated profile has two preferred values, roughly perpendicular to one another. This behaviour accounts for the low integrated polarization in the first component. Variable circular polarization can be seen in both components.

Some individual pulses have been recorded simultaneously at 408 and 240 MHz. There is a high correlation between the pulse shapes, states of polarization, and pulse widths, at these two frequencies.

PSR 1237+25. Individual pulses, recorded at 408 MHz, occur independently at two main pulse phases, corresponding to the peaks at the extremes of the integrated profile; a few pulses have also been recorded at an intermediate pulse phase. All pulses have a simple profile, with half-width 6 ms, practically fully linearly polarized. Circular components are seen, sometimes reversing during the pulse.

PSR 1642−03. Long sequences of single pulses have been recorded at 408 MHz; they have a consistent half-width of 4 ms. The intensity varies only slowly from pulse to pulse. All peaks occur within 3 ms, so that the integrated profile is more closely related to individual pulses than in any other pulsar we have studied.

No polarimeter records were obtained.

PSR 1749−28. Three individual pulses have been recorded on 408 MHz, bandwidth 300 kHz, using a RH circularly polarized antenna feed. The measured half-width was 6–7 ms. Allowing for dispersion, we assign a width of 6 ms to these pulses.

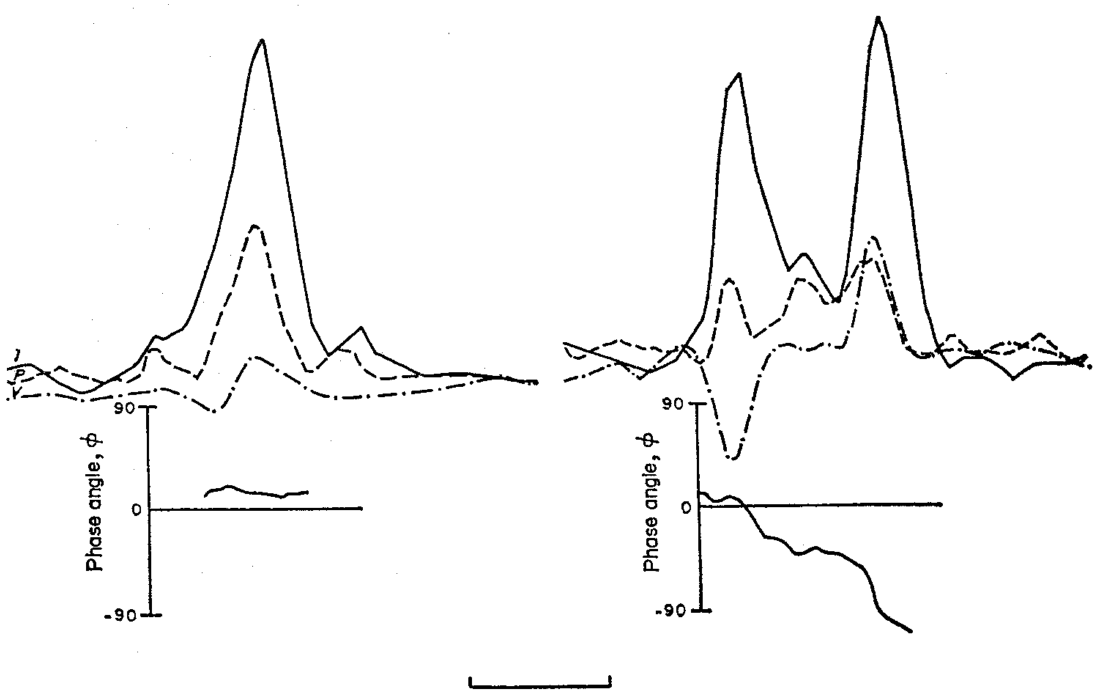

FIG. 6. *Two pulses from PSR 2016+28 recorded at* 408 *MHz, showing the independent appearance of individual pulses near the times of maximum of the integrated profile* (*see Fig.* 7). *The polarization is shown as the linear polarization, P* (– – – –), *the circular polarization, V* (–·–·–·) *and the position angle* ϕ.

PSR 1919+21. Individual pulses have only been recorded in total intensity (I) at 408 MHz. The typical width is 6 ms.

PSR 2016+28. This provides the clearest example of pulse drift. Fig. 6

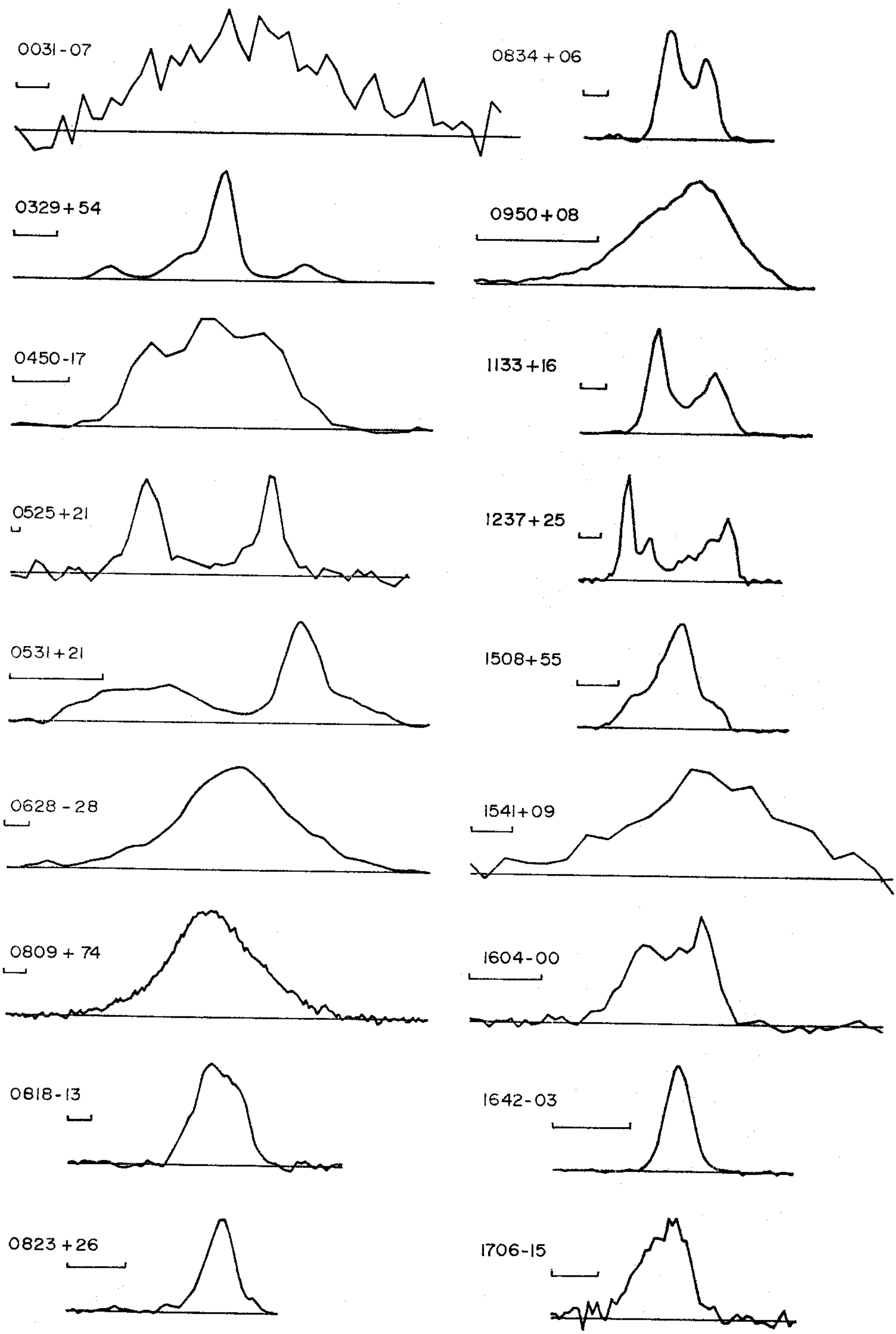

FIG. 7.

shows an analysis of two recordings, one with a single pulse and the other with two, showing I, V, $P = (Q^2 + U^2)^{1/2}$, and position angle. The individual pulses show the usual independent patterns of polarization, although the continuity of position angle across the pair of pulses is similar to that seen in the integrated profile.

PSR 2045−16. Recordings of intensity (I) at 408 MHz show isolated pulses 4 ms wide occurring at two locations, corresponding to the main peaks of the profile.

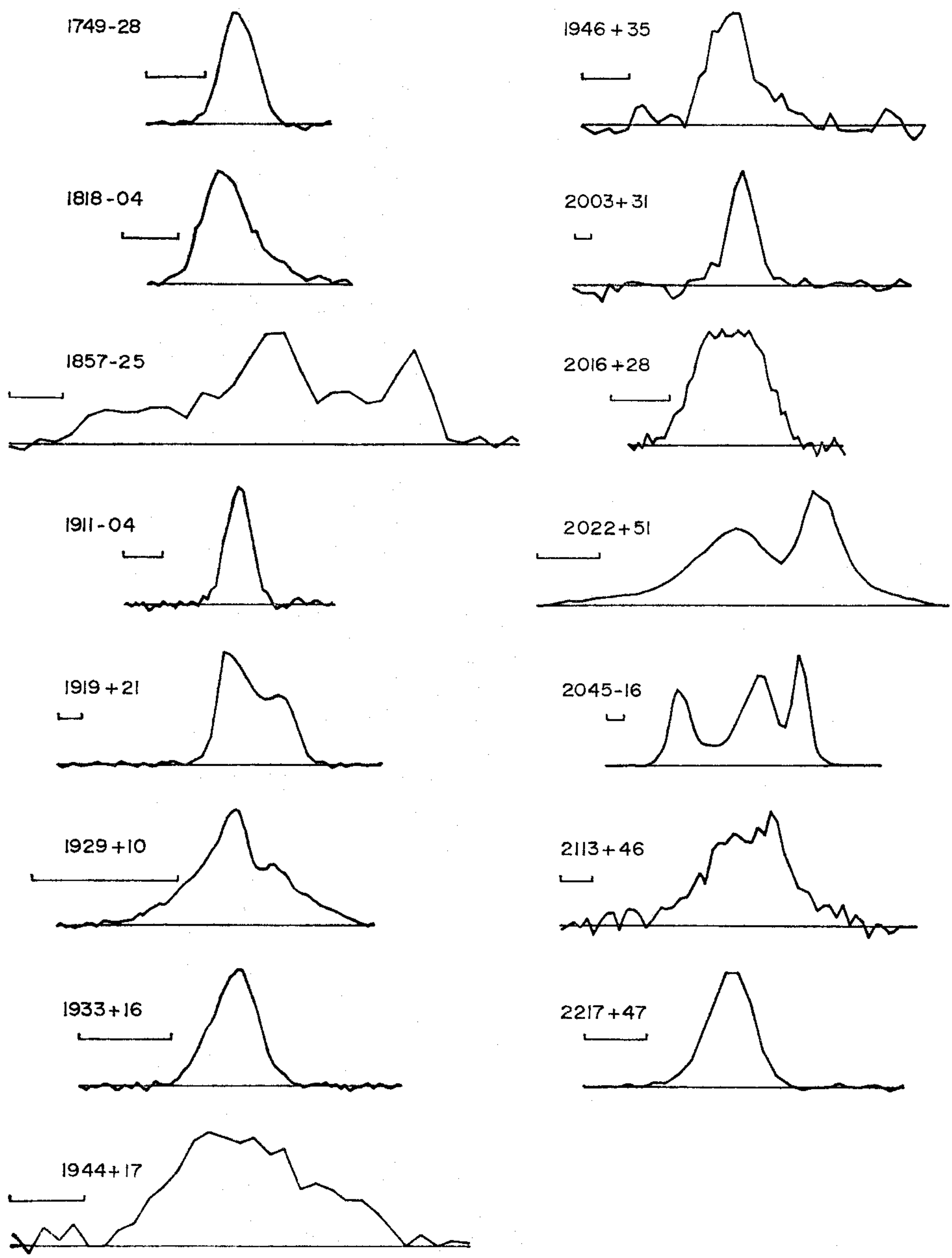

FIG. 7. *The integrated profiles of intensity, I, for* 33 *pulsars at* 408 *MHz. The heights are normalized to the same peak intensity, and the time scales are adjusted so that all profiles are on the same scale of rotational longitude. The actual time scales are indicated by a line representing* 10 *ms, except for PSR* 0531+21 *where the line represents* 1 *ms.*

5. THE TOTAL INTENSITY PROFILES

During the observations, an attempt was made to measure the profiles of the integrated Stokes parameter I for as many pulsars as possible at 408 MHz. On a number of pulsars, the observations were extended to 151 MHz, 240 MHz or 610 MHz.

The results at 408 MHz are shown in Fig. 7 in which the sources are arranged in order of increasing right ascension. A number of sources have been omitted in which the signal-to-noise ratios were poor. PSR 1845−04 and PSR 1858+03 have been omitted because of severe broadening attributed to multipath propagation in the interstellar medium (Davies *et al.* 1970; Drake 1971; Lyne 1971a). The profile for PSR 1946+35 is also affected by this at 408 MHz; the profile presented was obtained at 610 MHz and is almost free from this form of broadening.

Each integration was made over at least 10 min. Over this period of time, the pulse to pulse variations no longer affect the profile in a random way, and the profile is usually stable from one integration to the next. Two exceptions should be noted in that PSR 1237+25 and PSR 0329+54 both display a 'switching' phenomenon in which the pulse changes shape suddenly for some hundreds of pulses and then reverts to its more usual configuration (Backer 1970b; Lyne 1971b). The more usual configurations are shown.

The noise level in the diagrams varies considerably from one to the next and can usually be estimated from the ripple outside the region of the pulse.

The pulse broadening due to dispersion is usually less than the observational resolution, which itself is usually much finer than any structure in the profiles.

Fig. 8 shows how the profiles of a number of pulsars vary with frequency. In the pulsars PSR 0525+21, 1133+16 and 2045−16 the separations of the pulse components have already been shown to vary with frequency (Craft & Comella 1968; Komesaroff, Morris & Cooke 1970). For PSR 2045+16 we now see that both the front component and trailing component move inwards towards the centre one, at increasing frequencies. While the amplitude of the leading component remains the same with respect to the central one, the trailing one increases dramatically. (Note that Morris, Schwarz & Cooke (1970), observing at 2650 MHz, may not have resolved the trailing component.)

PSR 0329+54 behaves in a very similar way to PSR 2045−16. This source is also triple and the spacing of the components and their relative fluxes behave in a very similar fashion.

PSR 0950+08 and PSR 2016+28 both show very marked variations in profile with frequency. At low frequencies, the component at the front of the main pulse from PSR 0950+08 becomes very strong, while the trailing half of PSR 2016+28 almost disappears. The equivalent width of PSR 2016+28 decreases by nearly a factor of two between 408 MHz and 151 MHz.

The presently available information on the spectral variation of the separation of distinct components of the profiles is given in Table II, and plotted in Fig. 9(a). The quoted separations are the intervals between the peaks of the components, estimated by fitting a parabola to the top 10 or 15 per cent of the peaks. The quoted errors are rough estimates of the standard errors. It is seen that although no general law covers the behaviour of the component separation, there are several pulsars in which the separation decreases roughly as a low power of the frequency. In PSR 0834+06 and PSR 1919+21, however, the separation actually increases at higher frequencies. Fig. 9(b) shows the distribution of the indices, α, of the straight lines where the separation w of the components follows a law of the form $w \propto \nu^{\alpha}$.

The widths of the profiles of PSR 0823+26 and 0905+08, which appear to have only one component, also change appreciably with frequency; it is of course possible that for these pulsars the single component is actually made up of two superposed components whose relative position changes with frequency.

No other pulsar is known to show a profile which changes appreciably with frequency.

The widths of the integrated profiles have been tabulated in Table I in the form of equivalent widths, in which the area of the profile has been divided by the peak height. Profiles which are double or more complex may consequently have an equivalent width somewhat less than the spacing between their outermost

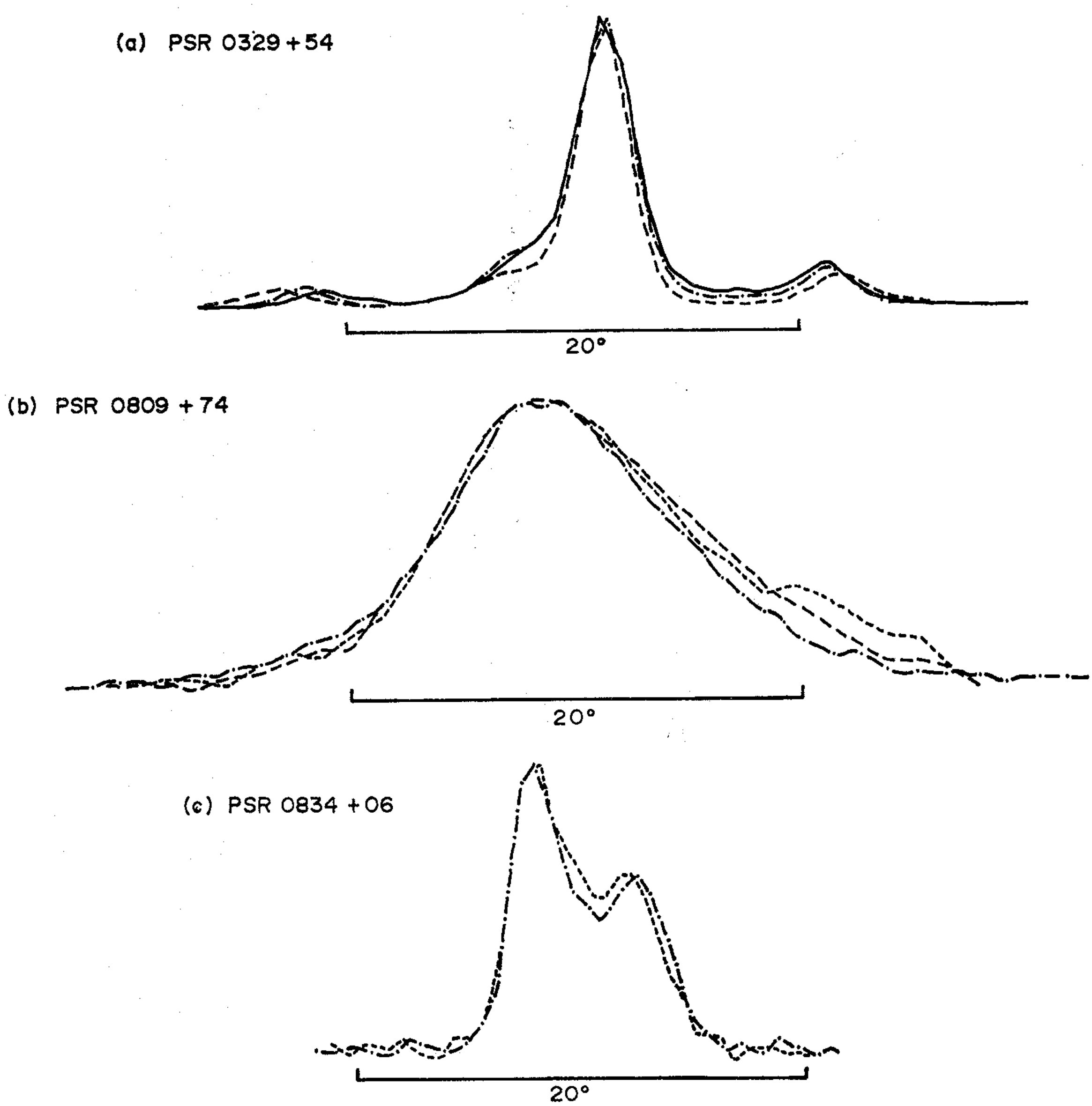

Fig. 8.

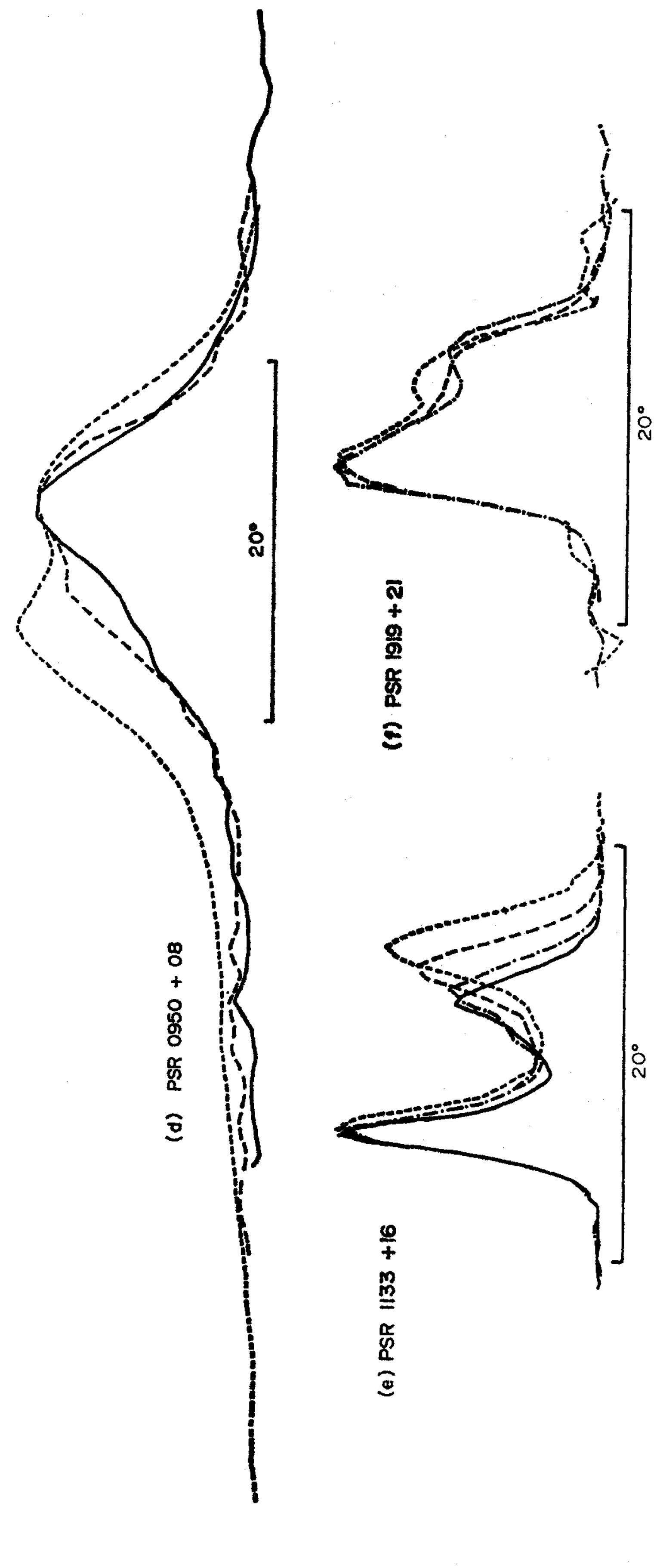

Fig. 8.

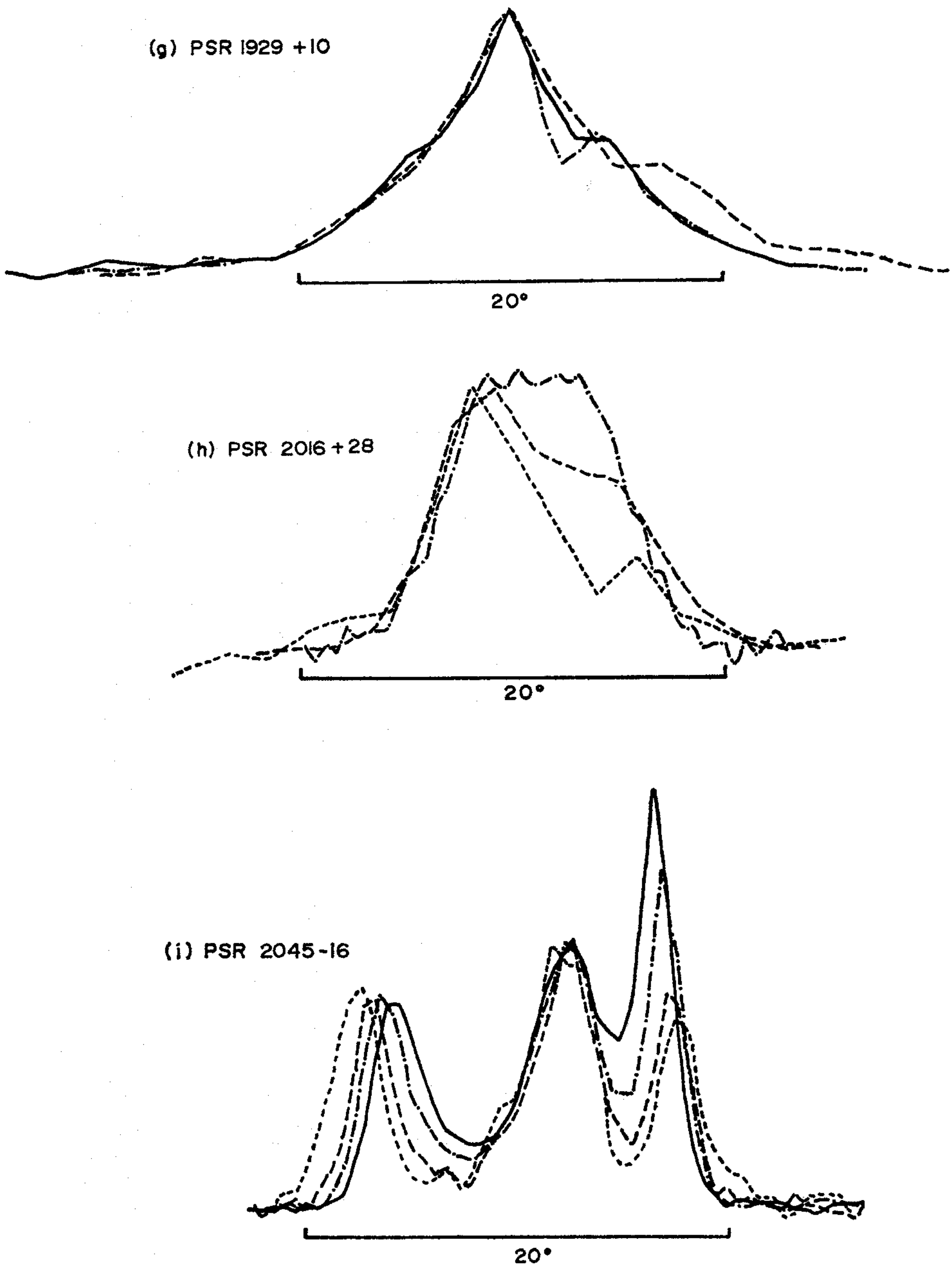

FIG. 8. *Variations of integrated pulse profile with radio frequency. The profiles at the four observing frequencies are shown thus:* ······ 151 *MHz*, ---- 240 *MHz*, -·-·- 408 *MHz*, ——— 610 *MHz*.

peaks. The equivalent width is quoted in milliseconds and in degrees of rotational longitude.

Fig. 10(a) shows these equivalent widths (in milliseconds) plotted against period, showing the familiar correlation of pulse width and period. The width expressed as a longitude is independent of period: for 19 pulsars with period less than 0·62 s the width is $11 \cdot 5° \pm 5 \cdot 5°$, while for 19 pulsars with period greater

Table II
Component separations

Pulsar	Frequency (MHz) 151	240	408	610	1420	2295	2695	α	Notes
0329+54a	15·8±0·4	14·7±0·4	13·5±0·4	12·3±0·4	11·0±0·5	—	—	−0·17	Leading outrider to main pulse.
0329+54b	—	10·5±0·2	10·0±0·2	9·7±0·2	—	—	—	−0·08	Trailing outrider to main pulse.
0525+21	—	—	—	—	11·1±0·5	—	—	−0·20	See Zeissig & Richards (1969).
0834+06	4·0±0·2	—	4·6±0·2	—	—	5·4±0·3	—	+0·11	—
1133+16	8·7±0·2	7·7±0·2	6·6±0·2	6·2±0·2	—	5·3±0·3	5·3±0·4	−0·17	—
1237+25	13·7±0·2	12·7±0·2	11·7±0·2	—	—	—	—	−0·15	Separation of outmost components.
1919+21	4·0±0·4	—	5·2±0·4	—	—	6·5±0·4	—	+0·18	—
2045−16a	9·9±0·3	9·2±0·2	8·6±0·2	8·1±0·2	—	7·3±0·3	7·1±0·4	−0·10	Leading outrider to central pulse.
2045−16b	5·4±0·3	4·9±0·2	4·6±0·2	4·2±0·2	—	3·3±0·3	3·2±0·4	−0·18	Trailing outrider to central pulse.

The data at 2295 MHz were obtained from diagrams presented by Ekers & Moffet (1968) and Ekers & Moffet (1969), and those at 2695 MHz from Morris, Schwarz & Cooke (1970). In Fig. 9(a), the data for PSR 0525+21 were obtained directly from Zeissig & Richards (1969). The point at 1420 MHz was obtained in the course of the present work.

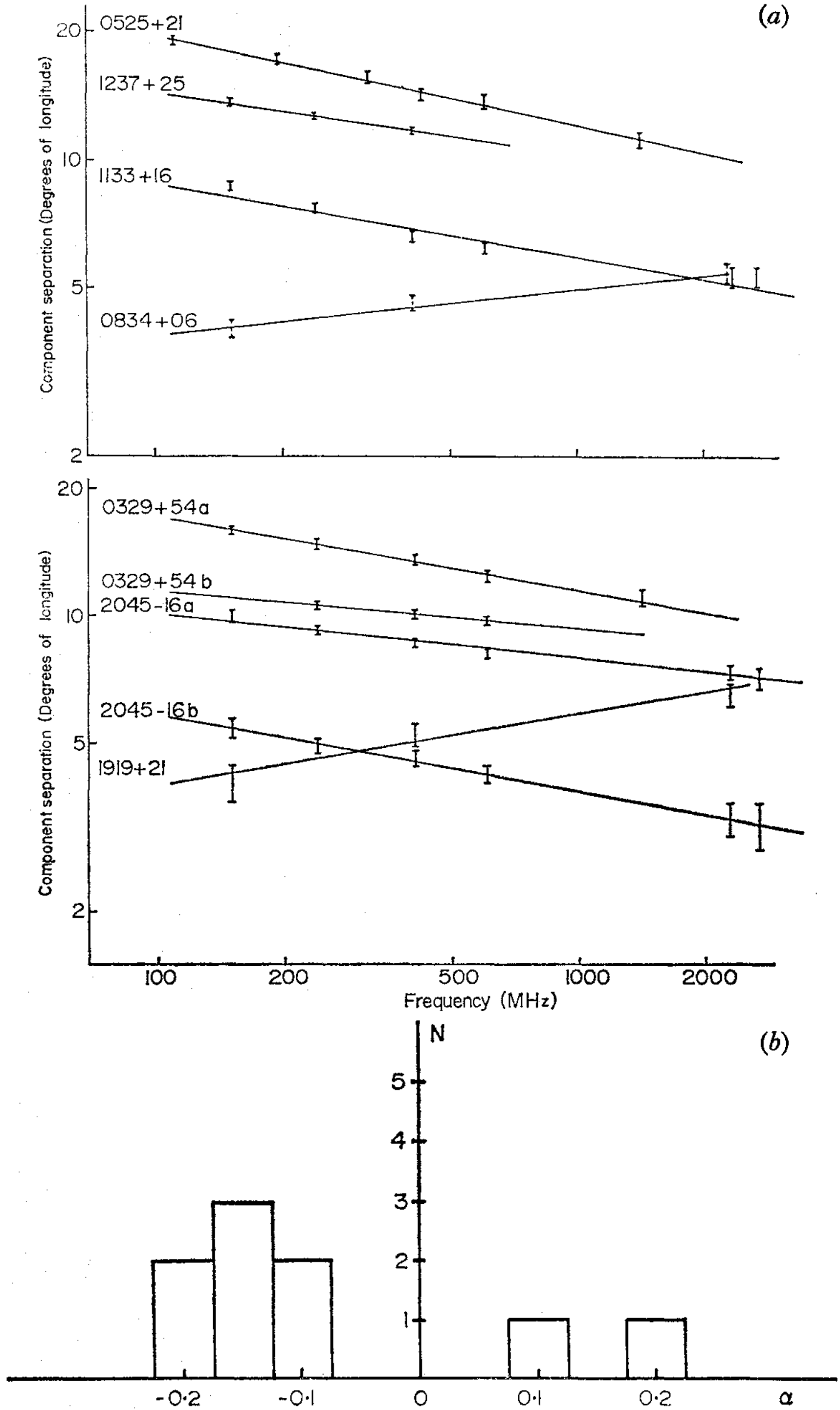

FIG. 9. (*a*) *Variations with frequency of the separation of components in the integrated profiles.* (*b*) *Histogram of the indices, α, derived from Fig.* 9(*a*).

than 0·62 s the width is $8{\cdot}5^\circ \pm 5{\cdot}5^\circ$ (standard errors). Fig. 10(b) shows the distribution of equivalent widths, expressed as longitudes, in the form of a histogram.

6. INTEGRATED POLARIZATION CHARACTERISTICS

A major part of our observation programme was directed towards obtaining the integrated polarization characteristics of a large number of pulsars at the

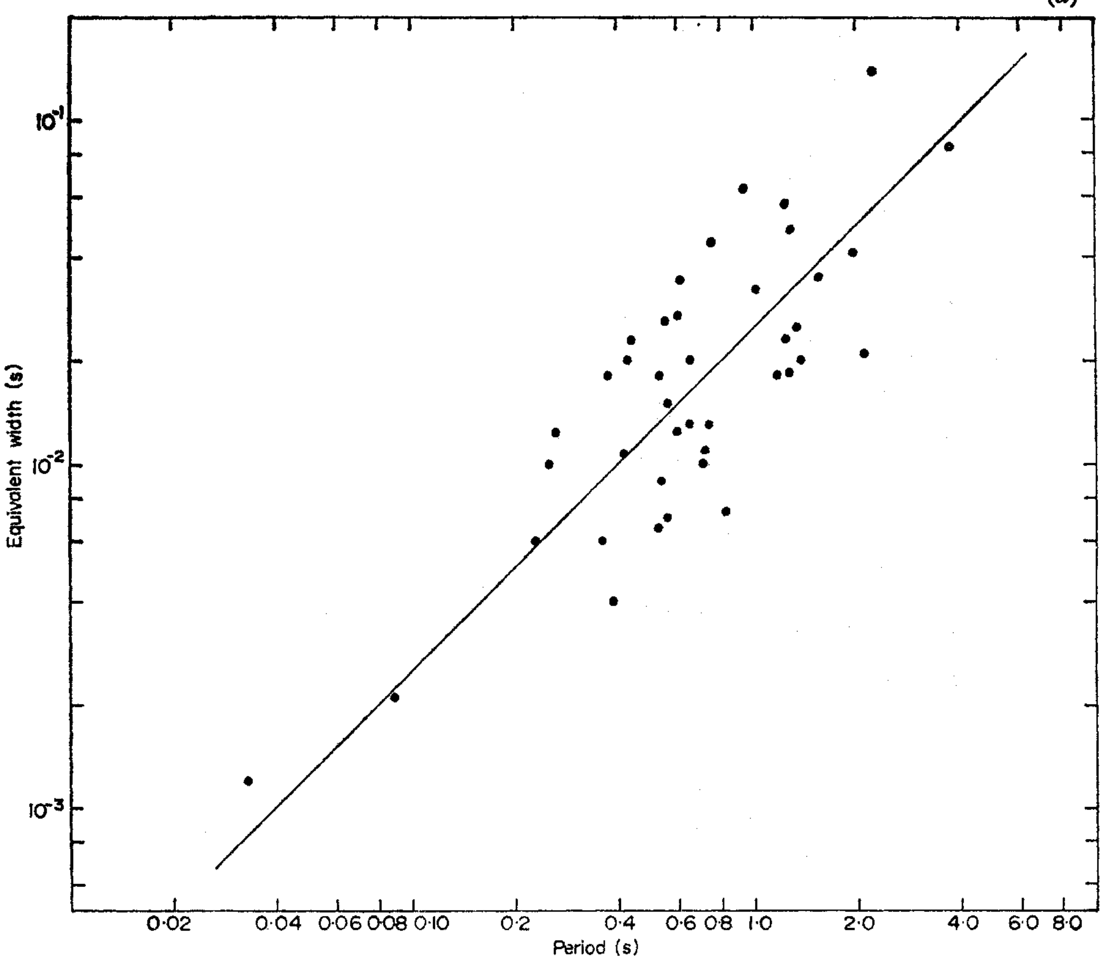

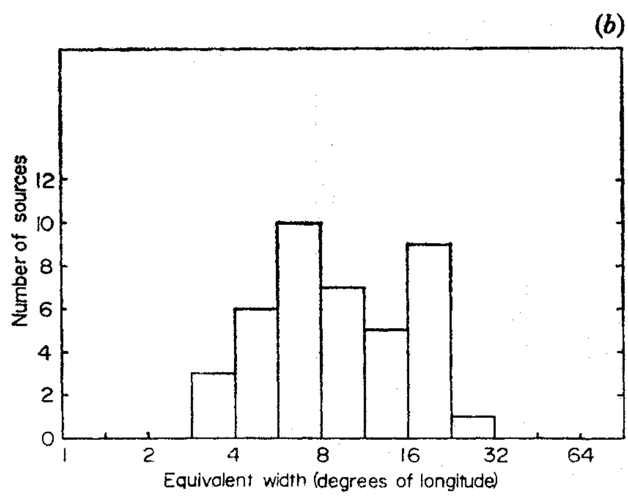

FIG. 10. *(a) The equivalent pulse width (s) as a function of period (s). The straight line is a line of constant width in longitude of 9·0°. (b) Histogram of the equivalent pulse widths in degrees of longitude.*

four radio frequencies, attempting in particular to obtain a complete set at 408 MHz. The integrations were extended over periods of between 2 and 60 min, according to the strength of the pulses; repeated observations were made to ensure that a representative profile had been obtained. Many of the results are presented in Fig. 11.1–34, which show integrated profiles of intensity *I*, the

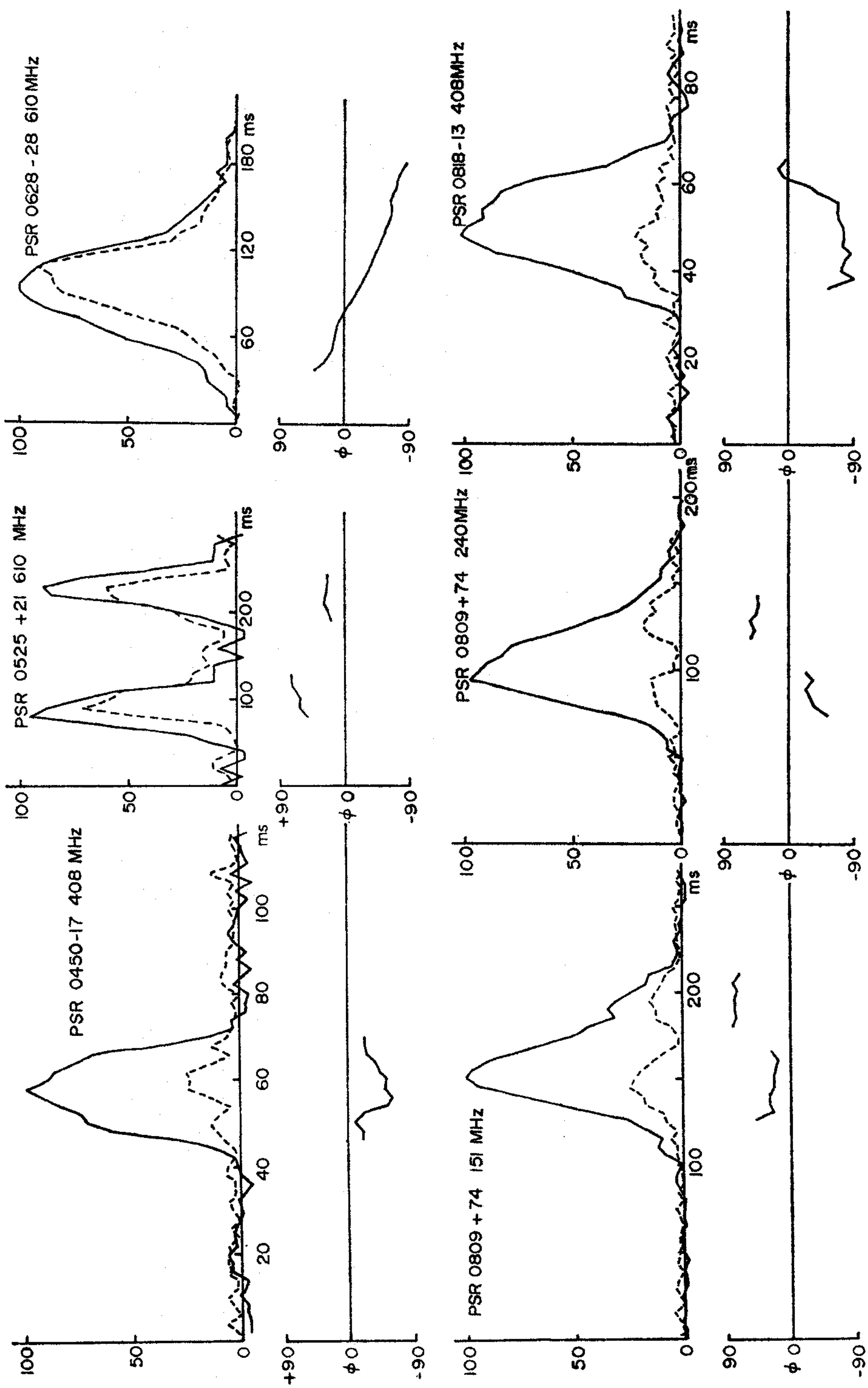

PSR 0450-17 408 MHz
PSR 0525 +21 610 MHz
PSR 0628 - 28 610 MHz
PSR 0809 + 74 151 MHz
PSR 0809+74 240MHz
PSR 0818-13 408MHz
ms

FIG. 11, 1–6

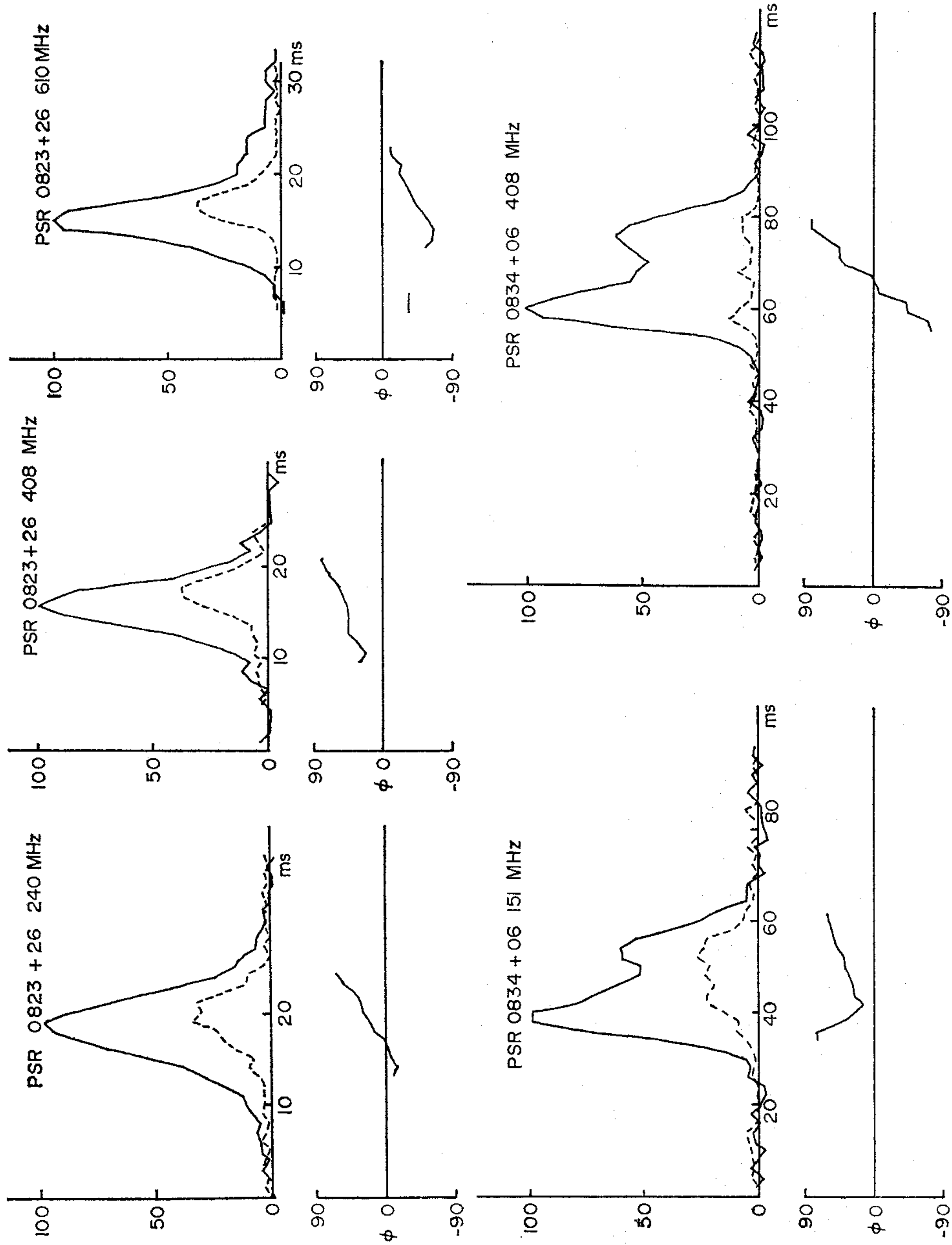
PSR 0823 + 26 240 MHz
PSR 0823+26 408 MHz
PSR 0823+26 610 MHz
PSR 0834 + 06 151 MHz
PSR 0834 + 06 408 MHz
100
50
0
ms
90
ϕ 0
-90

FIG. 11, 7–11

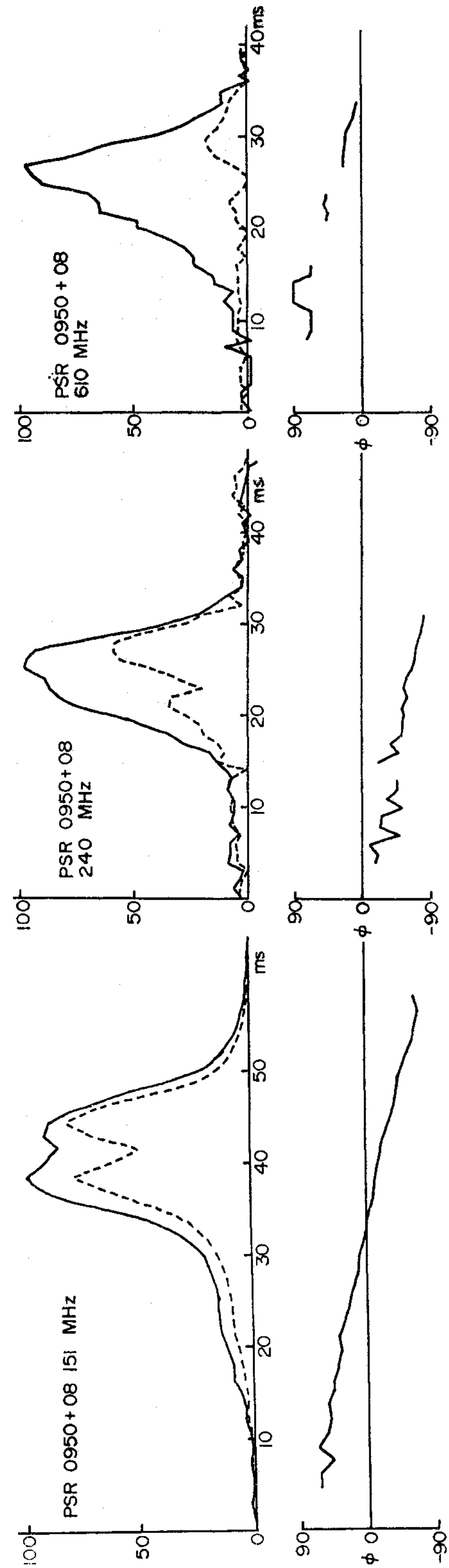
PSR 0950+08
610 MHz
PSR 0950+08
240 MHz
PSR 0950+08 151 MHz
100
50
0
90
0
-90
ϕ
10
20
30
40ms
40 ms
50
ms

FIG. 11, 12–14

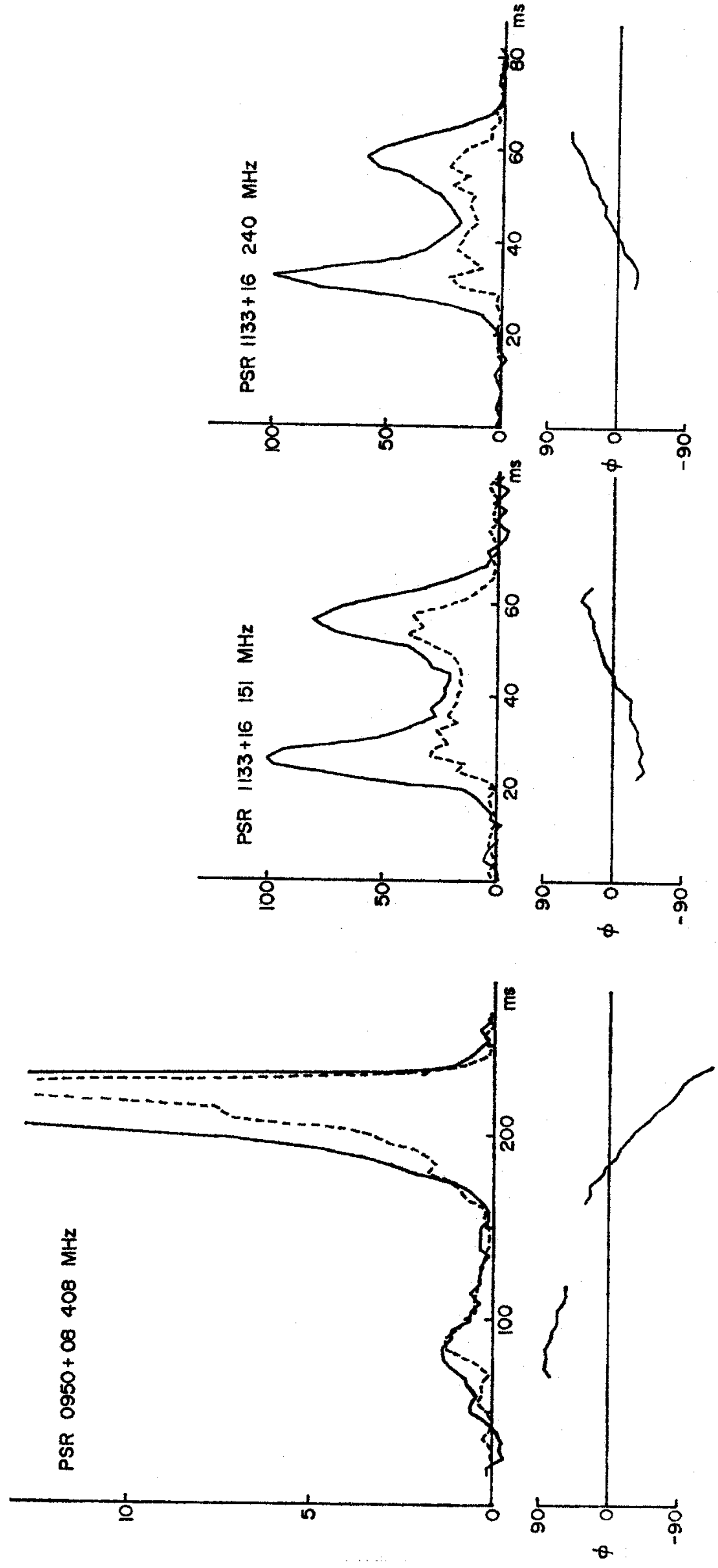
PSR 1133+16 240 MHz
PSR 1133+16 151 MHz
PSR 0950+08 408 MHz
ms
φ
0
20
40
60
80
100
200
50
5
10
90
-90

Fig. 11, 15–17

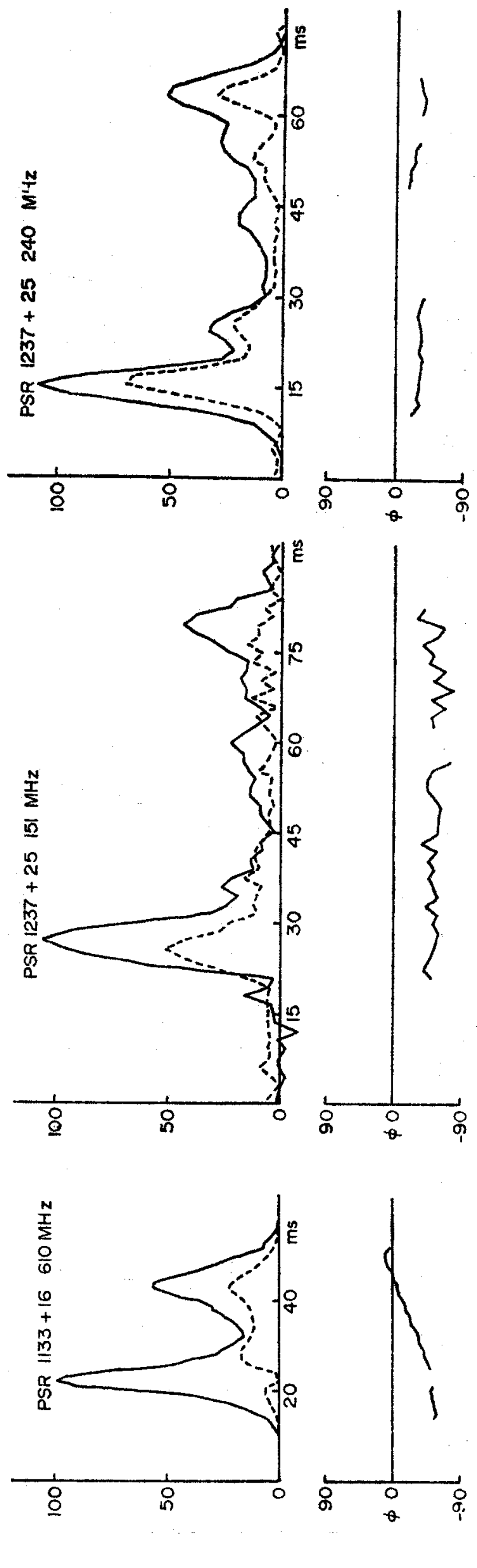
PSR 1237 + 25 240 MHz
PSR 1237 + 25 151 MHz
PSR 1133 + 16 610 MHz
100
50
0
90
φ 0
-90
15
30
45
60
75
20
40
ms

FIG. 11, 18–20

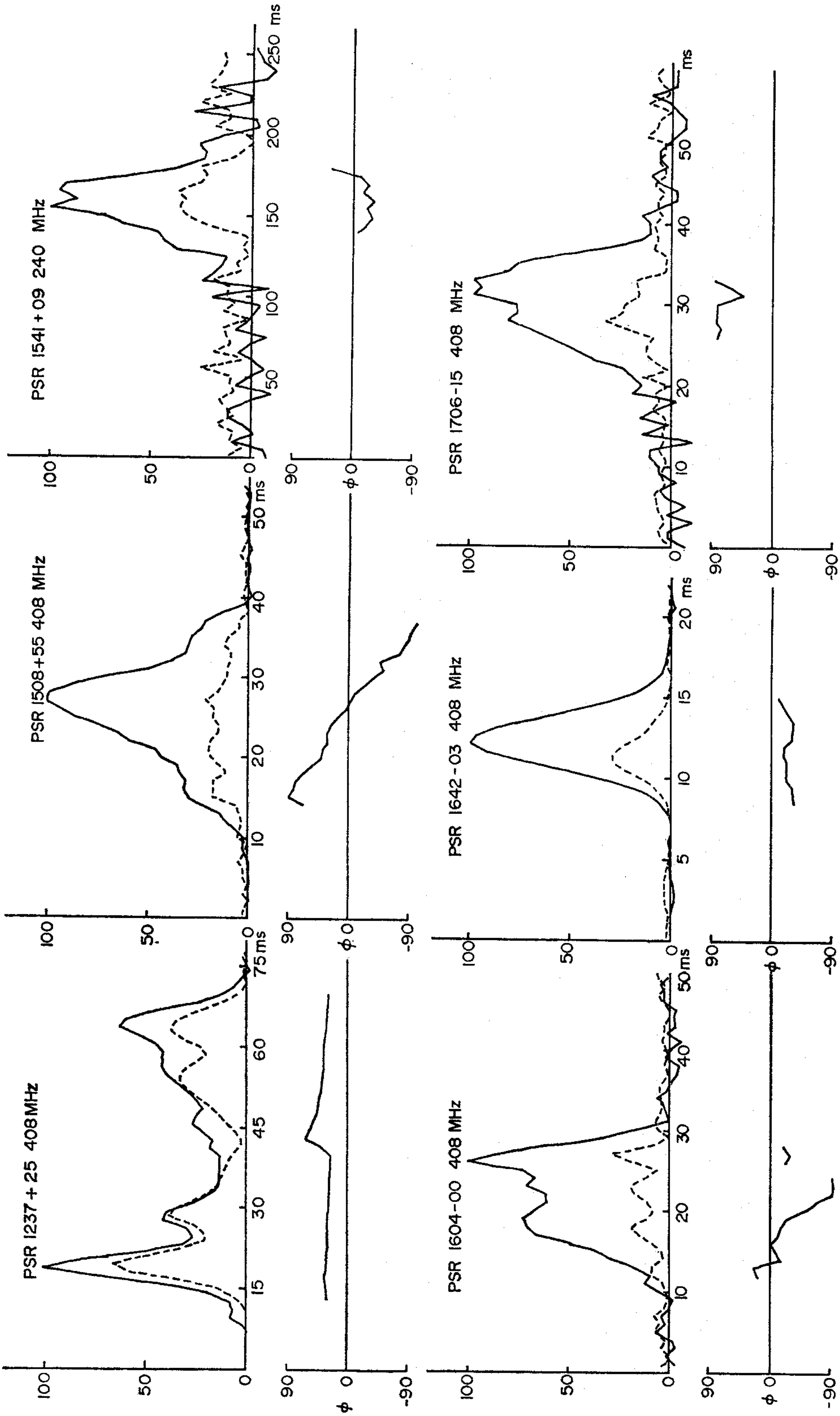
PSR 1237 + 25 408MHz
PSR 1508+55 408 MHz
PSR 1541 + 09 240 MHz
PSR 1604-00 408 MHz
PSR 1642-03 408 MHz
PSR 1706-15 408 MHz
75 ms
50 ms
250 ms
20 ms
ms
φ
90
0
-90
100
50

FIG. 11, 21–26

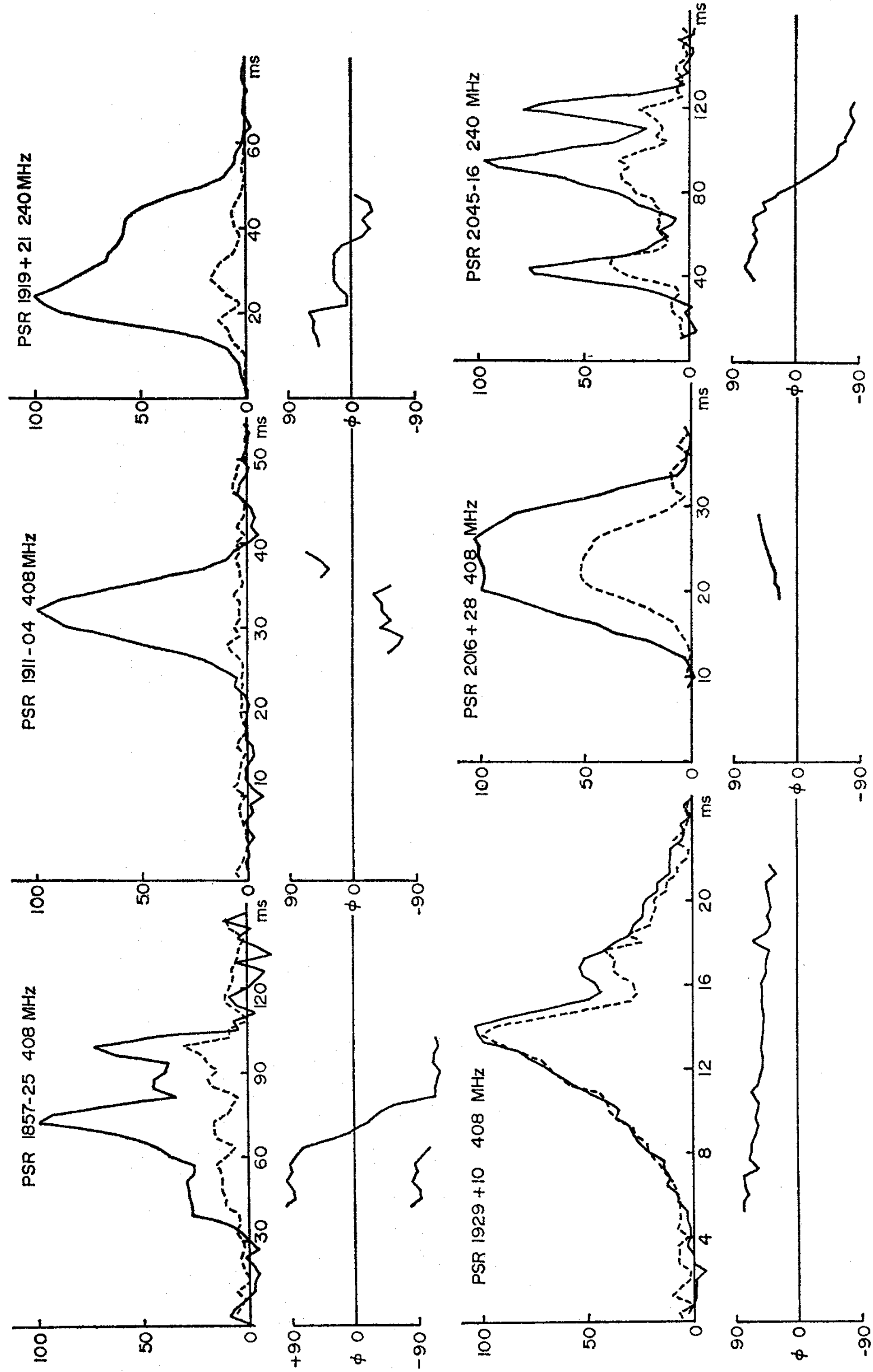

PSR 1919+21 240MHz
PSR 1911-04 408MHz
PSR 1857-25 408 MHz
PSR 2045-16 240 MHz
PSR 2016+28 408 MHz
PSR 1929+10 408 MHz
ms
ϕ

FIG. 11, 27–32

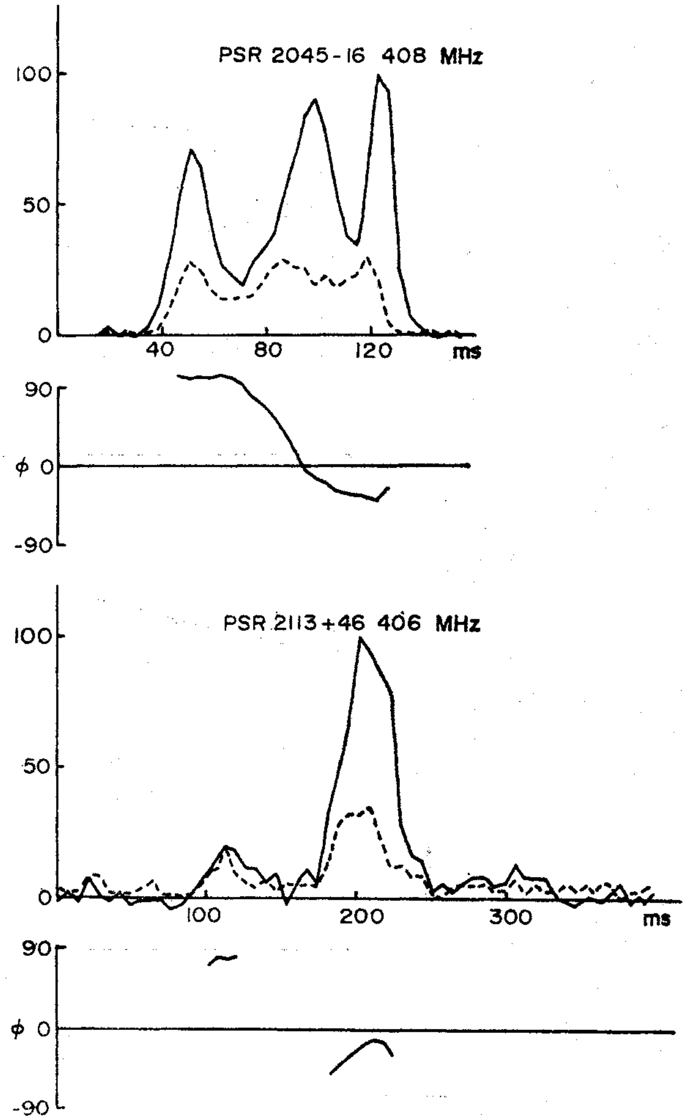

FIG. 11, 33–34

FIG. 11. *The integrated profiles showing the intensity, I, the linearly polarized component P (broken line) and the position angle ϕ.*

linearly polarized component $P = (Q^2 + U^2)^{1/2}$, and the position angle of polarization (ϕ). This position angle is measured according to the usual astronomical convention. No correction for ionospheric Faraday rotation has been made, and the zeros of position angle measurements are arbitrary. All the curves for I and P have been normalized to $I = 100$ at maximum.

The salient characteristics of pulse widths and polarization for all the observed pulsars are presented in Table I. The equivalent widths of the integrated profiles are quoted in milliseconds and in degrees of rotation (longitude). The half-width of the individual pulses was found from direct measurement of photographs; the only problem in interpretation here was found for PSR 0950+08, as already noted in Section 4.

The tabulated percentage linear polarizations are from ratios of the area under the curves of P and I. Peaks of polarization are often well above this value. The integrated circular polarization is usually smaller than the noise level, and only a few positive measurements have been noted in the Table. The swing of position angle through the integrated profile often contains a long and comparatively straight section; the extent and duration of this linear swing is tabulated, and the angular rate per degree of the pulsar cycle (i.e. per degree of rotational longitude in the source) is presented as a 'Phase Rate'. For some pulsars the variation of position angle is divided into several sections, which may be understood by reference to the curves in Fig. 11. The phase rate was usually measured from the 408 MHz records: where other frequencies were used a note appears in the Table.

The nomenclature of the pulsars incorporates some small changes resulting from recent more accurate measurements of their positions (Hunt 1971). Where the position is uncertain the original designation is used, as for MP 0835. The list includes all pulsars known up to February 1971.

Comparisons with measurements obtained elsewhere, which are referred to in the Notes, show generally a very good agreement. It is especially interesting to note that the general lack of variation of polarization characteristics with frequency, which appears in our measurements between 151 MHz and 610 MHz, extends to 2700 MHz for the pulsars PSR 0628−28, 1133+16, 1929+10 and 2045−16.

PSR 0950+08 provides a particularly interesting example of variation with frequency. The observations at 151 MHz and 240 MHz show a double profile with a high degree of polarization and a smooth swing of position angle through the interpulse and the main pulse. At 408 MHz and at 610 MHz the component separation is smaller; there is less polarization but the position angle follows the same swing. By contrast at 2650 MHz the position angle appears to swing in the opposite direction at a greater and more irregular phase rate; the polarization is still low and the pulse width is similar to that at lower frequencies. This behaviour is discussed in Section 9.5.

7. PULSAR PERIODS AND POSITIONS

During the observations, the declinations and periods of a number of pulsars were measured with a greater accuracy than in previous determinations. The declinations were measured at 408 MHz by a series of scans with the Mark I telescope at the known right ascension of the source. Two or more scans were made at such a speed that the telescope beam crossed the pulsar in a time short compared with the time scale of the fading of the pulsar radiation. The periods were obtained by continuous observation over a period of about half an hour; they were corrected for the Earth's motion and reduced to the corresponding periods at the barycentre of the solar system.

Table III summarizes the measured declinations and barycentric periods.

TABLE III

Measured declinations and barycentric periods

PSR	δ (1950·0)	P_b (s)
0450−17	−17° 50′ ± 10′	0·548 934 9 ± 5
0818−13	−13° 40′ ± 8′	1·238 124 5 ± 4
1604−00	−0° 23′ ± 8′	0·412 816 4 ± 2
1857−26	−26° 00′ ± 8′	0·612 208 3 ± 5
1911−04	—	0·825 933 9 ± 2
1944+17	17° 55′ ± 10′	0·440 617 9 ± 7

8. ROTATION MEASURES

The Faraday rotation of the plane of polarization in the interstellar medium is specified in terms of the rotation measure R, so that the total rotation at wavelength λ (m) is given by $\theta = R\lambda^2$ radians; R is given by

$$R = 0\cdot81 \int N_e H_{II}\, dl\, m^{-2}$$

where N_e is the electron density (cm^{-3}), H_{II} is the line-of-sight component of the magnetic field (microgauss), and the distance l is measured in parsecs. Since the dispersion measure D is $\int N_e\, dl$ (in the same units), the ratio $1\cdot24R/D$ gives a mean field $\bar{H}$, which is the mean field component along the line of sight weighted according to the electron density.

By observing a pulsar with considerable linear polarization successively at two or more adjacent frequencies the rotation measure can be obtained, and a mean field can be calculated (Smith 1968). At frequency ν (MHz) the difference $\Delta\theta$ is related to the frequency difference $\Delta\nu$ by:

$$\Delta\theta = -2R\left(\frac{300}{\nu}\right)^2 \frac{\Delta\nu}{\nu}.$$

We have measured $\Delta\theta$ for several pulsars, using frequency differences $\Delta\nu = \pm 2$ MHz at 408 or at 240 MHz depending on the expected magnitude of R. For some pulsars it is sufficient to measure θ for the average polarization over the whole integrated profile; the results of Section 6 show that for most pulsars the pattern of polarization is rather complex, so that it is necessary to resolve details of the pattern, thereby obtaining a sufficiently large polarization for a good measurement. Even then the rapid swing of position angle within the pulse may make the measurement difficult and dependent on accurate knowledge of dispersions. Our results are therefore rather limited, although the way now seems open to a more comprehensive set of measurements.

We present tables of the new results and a collection of the previously published determinations of rotation measures (Tables IV and V). These results are still too few for a detailed investigation of the Galactic magnetic field, but it is already interesting to look for any dependence of $\bar{H}$ upon D. The values of $\bar{H}$ (modulus) and D from the Tables are plotted in Fig. 12.

TABLE IV

Rotation measures (new determinations)

PSR	D cm^{-3} pc	R m^{-2}	$\bar{H}$ μG	Notes
1508	19·6	$+40\pm30$	$+2\cdot4$	The rapid swing of p.a. within the pulse makes the measurement difficult.
1642	35·7	$+48\pm10$	$+1\cdot6$	An ambiguity in the measurements allows also a value $R \sim +200$.
1929	3·6	≤ 4	$\leq 1\cdot4$	—
1933	159	-36 ± 10	$-0\cdot3$	This low value of $\bar{H}$ may be due to averaging over a large distance.
2113	~100	-182 ± 20	$-2\cdot2$	—

The two smallest values of D show low values of $\bar{H}$, possibly indicating a low field in the solar neighbourhood. If the line of sight to PSR 0950+08 is accidentally perpendicular to the local field, then that to PSR 1929+10 would be inclined at 50°; the upper limit at 1·4 μG is then not outstandingly small. Leaving aside these two low values, there is a tendency in Fig. 12 for $\bar{H}$ to fall at larger values of D. The fall is in accord with models in which the magnetic field is organized over large distances, with a typical structure corresponding to about 50 units of D, i.e. about 1 kpc if the electron density is 0·05 cm^{-3}. The actual field strength then would be about 3 microgauss throughout the Galactic plane.

Such conclusions must be treated with great caution. There is no reason for expecting to find the same value of magnetic field or the same size of structure close to and far from the Galactic plane, and the large values of D on which the argument depends are necessarily confined to low Galactic latitudes. There may

TABLE V

Rotation measures (previous determinations)

PSR	D cm^{-3} pc	R m^{-2}	H μG	References
0329	27	−65	−2·9	Smith (1968) Staelin & Reifenstein (1969) (see Note 1)
0525	50	+36	0·9	Staelin & Reifenstein (1969)
0532	50	−40·5 ± 3·5	1·0	Manchester (1971)
0628	35	45 +47	1·6	Vitkevich & Shitov (1970b) Schwarz & Morris (1971)
0808	5·8	12	1·7	Vitkevich & Shitov (1970a) (see Note 2)
0833	63	+42	0·8	Radhakrishnan & Cooke (1969)
0834	13	+26	2·3	Schwarz & Morris (1971)
0950	3·0	<0·5	<0·2	Smith (1968)
2015	14	−28	−2·5	Smith (1968)

Notes

(1) We adopt the numerical value from Staelin and Reifenstein, and the sign from Smith.

(2) The rotation measure for PSR 0808 has been obtained from Fig. 4 of the quoted reference on the assumption that the sinusoidal form of the spectrum is to be interpreted in the same way as for PSR 0628.

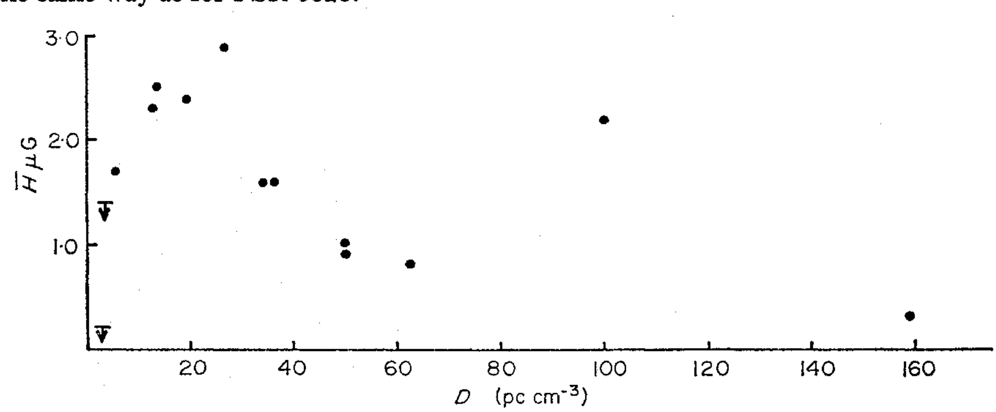

FIG. 12. *The mean field $\bar{H}$ (microgauss), obtained from the rotation measures, plotted against the dispersion measure D (pc cm^{-3}).*

also be serious selection effects: other pulsars with large values of D are needed at other Galactic longitudes before the present values of $\bar{H}$ can be accepted as typical.

Finally we note that PSR 2113+46, with $R = -182$, is only 3° from the extragalactic source 3C 431, with $R = +62$ (Berge & Seielstad 1967). This suggests that both results should be checked, although the fact that three other extragalactic sources, 3C 430, 3C 433 and 3C 452 lying within 20° of the same point all have large negative values of R tends to support the pulsar result. A comparison of values between PSR 1933 ($R = -36$) and three adjacent sources is not so clear cut; the sources are 3C 410 ($R = -216$), 3C 386 ($R = +79$), 3C 403 ($R = -34$), all about 15° from the pulsar.

9. DISCUSSION

9.1 *The individual pulses*

Our observations have led us consistently to the view that the radio emission from pulsars consists of elementary individual pulses which occur within a time 'window' defined by the integrated profile. The elementary pulses typically have a symmetric shape, like a Gaussian curve, and a width which is characteristic for each pulsar. They are fully polarized, generally elliptically; the state of polarization can change smoothly through the pulse. More than one pulse can occur within a single 'window', either separated by a characteristic distance or overlapping. This situation has been described by other authors in terms of a 'pulse', meaning a notional pulse with the shape of the integrated profile, and 'sub-pulses', which form the structure we have just described. We have avoided this nomenclature on account of the basic importance which we assign to the typical individual elementary pulses.

It has been suggested (Smith 1970a) that these individual pulses represent the basic beam of radio emission from a rotating pulsar; further, that the full polarization and the lack of dependence of pulse width on frequency together indicate that the beaming is a purely geometric effect. The relativistic beaming effect of a source driven to speeds of the order of 0·9 c by the co-rotating magnetosphere of the pulsar offers the only known mechanism for this. The pulse widths listed in Table I may accordingly be interpreted in terms of co-rotating sources moving with speeds between 0·85 c (PSR 0628−28) and 0·98 c (PSR 1133+16); the same fractions then represent their radial distances in terms of the radius of the 'velocity of light cylinder'.

9.2 *The integrated profiles*

Following the same interpretation, the integrated profiles now represent a range of longitudes which can contain the source of the beamed radiation. Across this range there is a variation of excitation, or probability of occurrence, which provides the shape of the profiles. There is a tendency towards symmetry in these profiles, which are generally of the following types:

(i) A smooth single hump, e.g. PSR 1642−03.
(ii) A double hump, e.g. PSR 1133+16.
(iii) A single hump with extensions or outriders, e.g. PSR 0329+54.
(iv) Double humps with structure between, e.g. PSR 1237+25.

The width is of the order of 3 per cent of the period, so that the longitude range is of the order of 5°→15°. The pulsars PSR 0531+21, 0950+08 and 1929+10 also have ‘ interpulses ’.

Each location within the profile has a preferred polarization; pulses occurring with that pulse phase may have a variable polarization, but there is usually a discernible average. Where the average polarization is low, it may be that more than one preferred polarization is to be assigned to that pulse phase, as in the first part of the double profile of PSR 1133+16. The polarization often varies smoothly through the profile; it may contain a component of circular polarization, which usually occurs where the linear component is small and where the position angle is changing fastest. A histogram of the linear polarization averaged through the profile is presented in Fig. 13. Although the polarization is for most pulsars

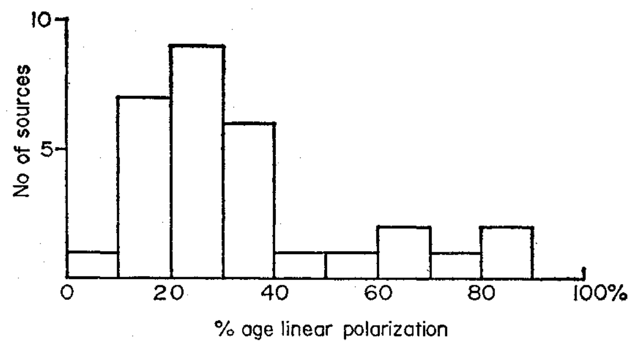

FIG. 13. *Histogram of the percentage polarization at* 408 *MHz, obtained from the areas under the integrated profiles of I and P.*

very similar over a wide range of frequencies, some pulsars show changes which are usually associated with changes in the intensity profiles. For example, PSR 0950+08 and 1642−03 show a fall of polarization with increasing frequency, together with a narrowing of the profile, while PSR 1508+55, 1237+25 and 2045−16 show an increase of polarization with increasing frequency.

9.3 *The position angles within the profile*

9.3.1 *Relation to a single vector.* It has been pointed out by several authors (Wampler, Scargle & Miller 1969; Radhadkrishnan & Cooke 1969) that the sweep of position angle within a short section of the profile may be related in a simple way to a defined direction rotating with the pulsar. For example, that direction might be a magnetic field line above a magnetic pole; if the maximum emission is observed when the pole crosses the observer's meridian, the maximum rate of sweep of position angle is then mainly determined by the minimum angular distance θ between the pole and the line of sight. On this model the maximum ‘ phase rate ’ $d\phi/dl$ is related to θ by

$$\frac{d\phi}{dl} = \frac{\sin D}{\sin (D-\theta)}$$

where D is the angle between the rotation axis and the magnetic axis. Since the phase rate does not depend critically on D, provided that D is not near zero, it is convenient to put $D = 90°$ and evaluate θ from

$$\frac{d\phi}{dl} = -\operatorname{cosec} \theta.$$

24§

The interpretation in this way of the whole of the observed swing of position angle in terms of a single parameter θ is evidently insufficient for most pulsars; indeed it is often difficult to choose a suitable single value of phase rate as representative of a given pulsar. There is a strong suggestion that many of the profiles are made up of two or more independent components, which might be interpreted as separate longitude regions where emission might occur. Two separate components are seen in PSR 0525+21, for example, with different position angles, each component having a low phase rate. In PSR 0809+74 there may be two components, not so clearly separated in the intensity profile but distinguishable by the step in the position angle. If two such components overlap, the position angle would sweep monotonically from one value to another, while the polarization would be minimum at the time of most rapid sweep.

For each pulsar we have chosen a single phase rate, which represents the longest range of longitude over which there is a consistent swing. These are plotted as a histogram in Fig. 14. The phase rates have been converted into inclinations θ and plotted in the histogram of Fig. 15. (It should be noted that values of θ greater than about 30° obtained in this way have little meaning, on account of the assumption that $D = 90°$.)

We comment generally on this interpretation of the phase rates in Section 9.4, but we suggest here that only the low values of phase rate should be used in such an analysis, since the five pulsars with the largest phase rates (> 15 in Fig. 14) all show complex profiles which could contain overlapping components. Furthermore, none of these profiles shows a high degree of polarization, even though the individual pulses of two of them have been observed to be fully polarized.

At the lower end of the histogram of phase rates, the profiles are generally

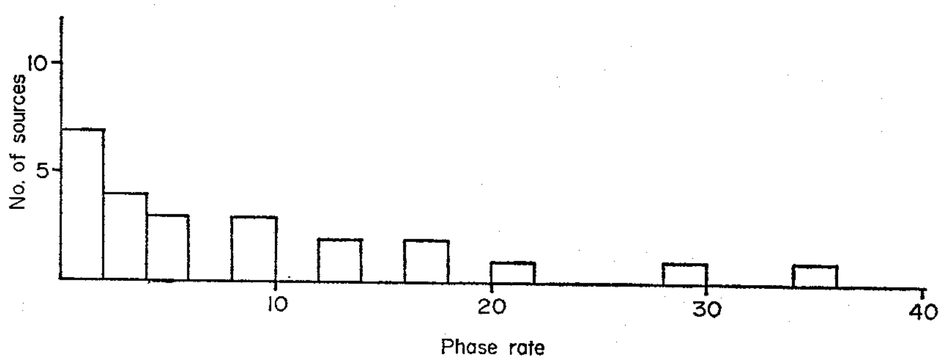

FIG. 14. *Histogram of the rate of swing of polarization position angle, expressed as a phase rate $d\phi/dl$.*

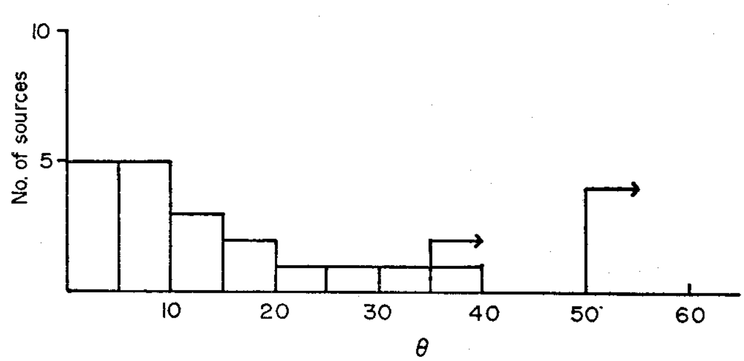

FIG. 15. *Histogram of the minimum angle θ between the observer's line of sight and the magnetic field axis, according to the interpretation of Section 9.3.1.*

either smooth, or contain well-separated components. The highest degrees of polarization are found amongst the pulsars where the phase rate is less than 6.

We suggest therefore that

(i) a typical component has a phase rate of less than 6, corresponding to an angle θ greater than about 10°,
(ii) a step in position angle can separate distinct components, which often have similar phase rates,
(iii) large phase rates may be due to the presence of overlapping components with different position angles.

According to this interpretation, PSR 1919+21 may contain three components, as suggested by the polarization characteristics of Fig. 11.29, rather than two, as appears in the profile of intensity above.

The separate components may have different spectra, as seen in several profiles where they are well separated in time. Where they overlap, the polarization characteristics may then become markedly dependent on frequency. This would, for example, explain the very different behaviour of PSR 0834+06 at 151 and 408 MHz, as seen in Fig. 11.10 and 11.11.

The rapid swing of position angle in the centre of the profile of PSR 1237+25 may, however, be of a different kind, since it is at this point of the profile that an unusually large value of circular polarization is observed. The graph of position angle in Fig. 11.21 suggests that the rotation may even amount to 180° at this point; we suggest that this behaviour results from a close alignment between a magnetic axis and the line of sight. This is discussed further in Section 9.5.

9.3.2 *Relation to a rotating magnetic field.* An alternative to the model outlined in Section 9.3.1 is to associate each part of the integrated profile with a definite longitude, so that the profile represents the successive passage of different emitting regions through a region from which their radiation can be observed. This region might be tangential to a circular motion near the velocity of light circle; Gold (1969) suggested that the radiation from such a region might be a consequence of the circular motion itself, while Smith (1970a) suggested that the emission occurred even within the rotating frame of reference, and that the observed radiation was the result of a relativistic Doppler effect at this tangential point. The progress of the emitting source through the defined region then brings to the observer a changing view of a rotating magnetic field, and the polarization will rotate according to the departure of the field from the radial direction.

For simplicity we consider first a rotating dipole field, and we suppose that the radiation originates from a tangential point in the equatorial plane. An observer whose line of sight makes an angle α with the rotation axis will see a projection of the magnetic field lines, as in Fig. 16. Then the rate of change of position angle of the field lines at P (the phase rate) is

$$\frac{d\phi}{dl} = -\frac{\cos\alpha}{2\cos^2 l + \frac{1}{2}\sin^2 l \cos^2\alpha}$$

where l is measured from the magnetic axis. It should be noted that ϕ is a monotonic function of l, with the rate $d\phi/dl$ varying between $-(2/\cos\alpha)$ and $-(\frac{1}{2}\cos\alpha)$ but never reversing. Further, the rotation of position angle is in the opposite direction to the rotation of the star. The maximum phase rate occurs where the field lines are tangential, i.e. 90° in longitude away from the dipole axis.

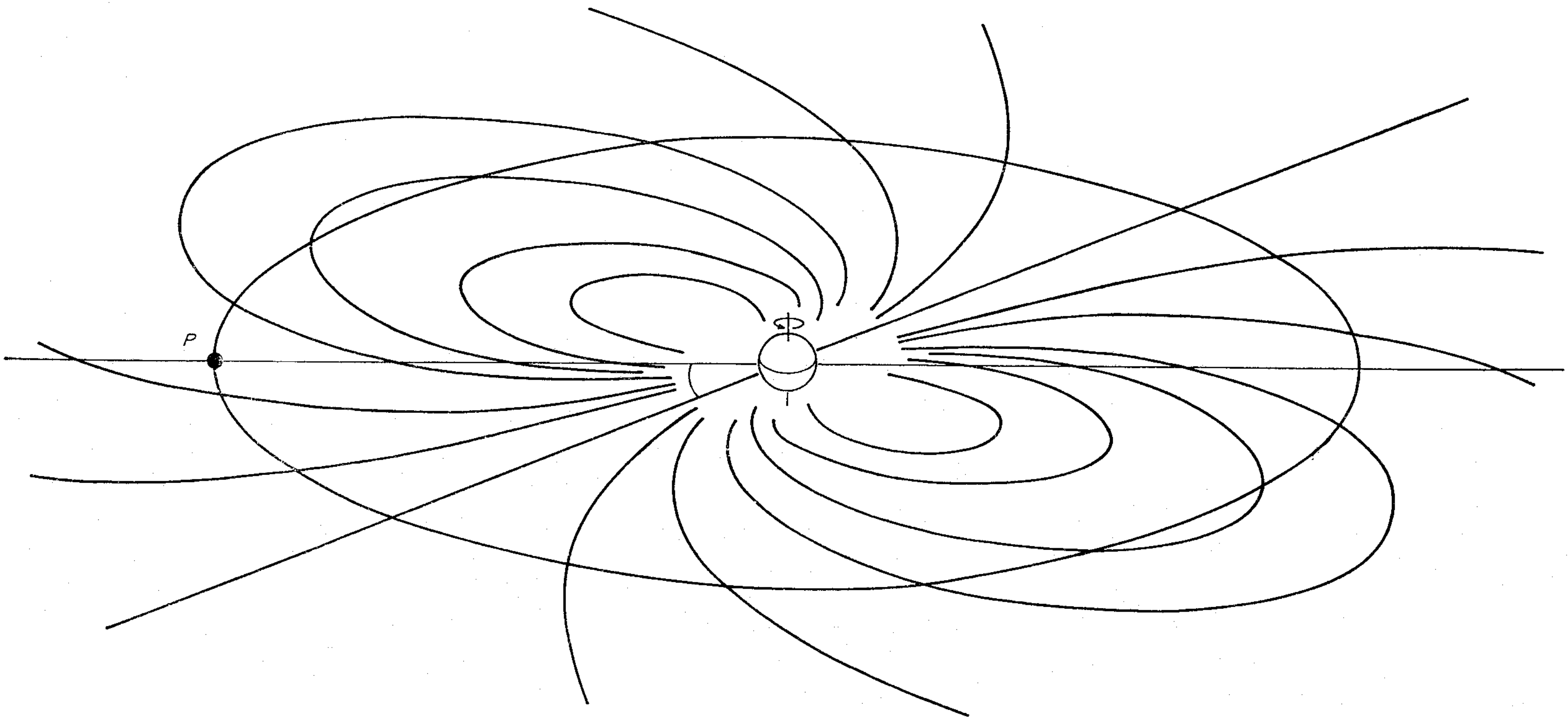

Fig. 16. *Magnetic field lines originating in a dipole whose axis is perpendicular to the rotation axis. The field direction rotates at an emitting region, such as the tangential point P, which is fixed in the observer's frame of reference.*

The configuration of the field is expected to be dipolar only close to the surface of the star. If the emitting region is at a distance from the neutron star approaching the radius of the velocity of light cylinder, the field lines at the source will be swept back through an angular distance approaching one radian. The topology is, however, unchanged, and ϕ will still be a monotonic function of l, while the phase rate varies through a larger range. The field configuration will be further distorted by plasma flowing out from the star, and there may be sufficient local distortions of the field to obscure the underlying monotonic sweep of position angle.

9.4 *Comparisons with the observed sweep of position angle*

9.4.1 *The simplest pulsars.* The clearest comparisons between theory and observation must concern the pulsars with simple profiles and high degrees of polarization, i.e. PSR 0628−28, 0833−45 and 1929+10. These have swings of $+110°$, $-95°$ and $-35°$ respectively, at phase rates of $+2\cdot5$, -5, and $-1\cdot3$.

The simple vector approach of Section 9.3.1 leads to inclinations θ of 24°, 12° and 50° respectively. This large range makes it difficult to construct a model in which the pulses are formed by a beam of emission related solely to the configuration of the magnetic field lines near a magnetic pole.

In the alternative approach of Section 9.3.2 the beam is formed by the relativistic motion of the source, and the sweep of position angle reflects the changing configuration of the field through a range of longitude. In the three pulsars under discussion the position angle varies smoothly through the profile. This suggests that the field has a simple configuration at the emitting region. The modular phase rates of all three are greater than unity, suggesting that the emitting regions are located at those longitudes where the magnetic field lines are tangential rather than normal to the velocity of light circle.

On this interpretation the field lines may be approximately dipolar, and not much distorted by the flow of plasma from the star.

9.4.2 *PSR 0950+08 and other pulsars with interpulses.* The swing of position angle in the profile of PSR 0950+08 can be traced from the interpulse right through to the end of the main pulse, representing a total monotonic swing of 210°. It is important in both interpretations that a swing greater than 180° has been observed, since it is then impossible that the line of sight can be further from the rotation axis than is the magnetic axis: otherwise there would be a rocking of the position angle rather than a continuous rotation. If the beam is formed by the relativistic process, the observer's line of sight must be within about 25° of the equatorial plane (Smith 1970a): we deduce therefore that the dipole axis is inclined less than 25° to the equatorial plane.

PSR 0950+08 is also important because of the existence of the interpulse which is almost, but not exactly, halfway between successive main pulses. Only two other pulsars, PSR 0531+10 and 1929+10, are known to have interpulses, although the present observational accuracies still allow their existence at a level of about 1 per cent for the majority of pulsars. Models of pulsars must therefore account for asymmetry in the emissivity of a magnetosphere in which the field has so far been assumed to be symmetrical, even if not dipolar.

If the beaming were explicable in terms of a magnetic field configuration near a pole, then it would be natural to explain the asymmetry by suggesting that the dipole axis is inclined to the equatorial plane, and that one end of the axis crosses the line of sight of the observer. If this were so, then to account for the interpulse in PSR 0950+08 one must suppose that both poles in turn approach the line of sight. In such a configuration, however, the position angle would swing rapidly both during the main pulse and the interpulse, which does not occur. Evidently the asymmetry must be of another kind.

There are two further observed asymmetries to be accounted for. First, the phase rate is smaller in the interpulse than in the main pulse. Second, the interpulse is not symmetrically placed. The second can be accounted for in terms of the difference of light travel time from two separate locations on a light cylinder which is inclined to the line of sight. The asymmetry in the phase rates seems, however, to indicate a real asymmetry in the configuration of the field; presumably the asymmetry in the emissivity is closely related to this.

9.5 *The sense of rotation of the pulsars*

The two models outlined in Sections 9.3.1 and 9.3.2 give opposite senses of rotation of the position angle relative to the rotating magnetic field. If the emission is related to a vector rotating with the star, then the position angle rotates in the same sense as the star: if the emission is from a succession of field lines crossing a location which is fixed relative to the observer, then the rotation is opposite.

It seems possible that the observed rotations could be associated with either hypothesis, even if the pulses were formed entirely by the beaming hypothesis. Suppose that the emitting region was confined to a very small range of longitude, so that the width of the profile was determined only by the width of the superposed individual pulses. Then the plane of polarization would be determined by the position angle of the field at that longitude only, and it would rotate with the star. If instead the longitude range was much larger than the angular width of a single pulse, the rotation would be in the opposite sense, as discussed in Section 9.3.2.

There are possibly two examples of pulsars with phase rates that are opposite in sign at different frequencies. At frequencies of 610 MHz and below the pulsar PSR 0950+08 has a negative phase rate, while the observations of Komesaroff *et al.* at 2650 MHz and Ekers & Moffet at 2295 MHz show a positive phase rate. The shape and width of the profile is also notably dependent on frequency. If these phase rates are indeed opposite, then the emission at higher frequencies could possibly be confined to a sufficiently small range of longitudes as compared with that at lower frequencies for the reversal to be explicable in the terms of this discussion.

The other possible example is PSR 0531+21, the Crab Nebula pulsar. Schonhardt (1971) has reported a swing of position angle at 408 MHz in the opposite sense to that observed optically. Since it is very likely that the emission at optical and radio wavelengths has a different physical origin, even though the locations of the two sources coincide, it is quite possible for the extent of the sources to differ sufficiently for the same geometrical difference to apply.

The appearance of circular polarization in the integrated profiles of some pulsars may be related to the same geometrical considerations. PSR 1237+25 is a pulsar in which the individual pulses are much narrower than the integrated profile, so that the general steady swing of position angle should reflect the change of field direction. In the centre of the profile there is, however, a rapid swing of position angle and a large value of circular polarization (V), both lasting not much longer than the length of an individual pulse. It is suggested that at this point the magnetic pole crosses very close to the line of sight of the observer, and the consequent rapid swing of position angle of the field line at the point of emission becomes the dominant factor for a short while. The appearance at the same point of a high degree of circular polarization adds some weight to this suggestion.

9.6 *The pulse profiles and the emission spectrum*

The association of a definite longitude with each point on a pulse profile provides a satisfactory explanation of the general independence of the shape and width of the profiles on frequency. The changes that have been noted in Section 5 are, however, well organized and very similar over a number of pulsars, and they merit some further discussion. Movements in longitude of components of the profiles might be interpreted as changes in the direction of an emitted beam of radiation; we prefer to associate the individual pulses with such a beam, and we do not pursue this line of argument. Instead we suggest that the spectrum of the emission at any point may cover a limited frequency range, of the order of one octave only, so that different frequencies may be emitted from points with a definite physical separation. There could, for example, be a close relation between emitted radio frequency and strength of magnetic field: then different frequencies would be emitted along a line of field gradient. If the configurations of the magnetic field lines were similar for several pulsars, then their changes of profile would also be similar.

A relation of this sort would, of course, only apply if the field configuration were essentially fairly simple. The simple behaviour of position angle through the profile for many pulsars suggests that this is indeed the case. The field may nevertheless be considerably distorted from a pure dipolar configuration; for example it could follow a trailing pattern such as that outlined by Endean & Allen (1970).

For those pulsars where there is little or no change of profile with frequency the position of the emitting regions may still vary, provided that it does not vary over a large range of longitude. The gradient of field may then be more nearly parallel to the rotation axis, rather than in the equatorial plane.

If this geometrical model is correct, there is a clear implication that the radiation mechanism is not as wide-band as had previously been suggested (Lyne & Rickett 1968). Recent observations of intense individual pulses from the Crab Nebula pulsar at frequencies near 100 MHz (Heiles & Rankin 1971) suggest that their spectrum covers a range $\Delta f/f \sim 0{\cdot}3$. Some further observations of individual pulses over a wide frequency range in other pulsars would clearly be of value in establishing the bandwidth of the fundamental emission process.

ACKNOWLEDGMENTS

We are grateful to many colleagues who have helped with these observations, and in particular Dr B. J. Rickett, Dr M. I. Large and Mr G. C. Hunt. The photographic technique was developed and used first by Dr R. R. Clark. The most important contribution has been made by Professor J. G. Davies, who provided the excellent facilities for the on-line computations.

University of Manchester, Nuffield Radio Astronomy Laboratories, Jodrell Bank

REFERENCES

Ables, J. G., Komesaroff, M. M. & Hamilton, P. A., 1970. *Astrophys. Lett.*, **6**, 147.
Backer, D. C., 1970a. *Nature*, **228**, 752.
Backer, D. C., 1970b. *Nature*, **228**, 1297.
Berge, G. L. & Seielstad, C. A., 1967. *Astrophys. J.*, **148**, 367.
Born, M. & Wolf, E., 1965. *Principles of Optics*, 3rd ed. Pergamon Press Ltd, Oxford.
Clark, R. R. & Smith, F. G., 1969. *Nature*, **221**, 724.
Cole, T. W., 1970. *Nature*, **227**, 788.
Craft, H. D. & Comella, J. M., 1968. *Nature*, **220**, 676.
Davies, J. G., Large, M. I. & Pickwick, A. C., 1970. *Nature*, **227**, 1123.
Davies, R. D., Ponsonby, J. E. B., Pointon, L. & Jager, G. de., 1969. *Nature*, **222**, 933.
Drake, F. D. & Craft, H. D., 1968. *Nature*, **220**, 231.
Drake, F. D., 1971. *Proc. I.A.U. Symp. No.* 46, Reidel.
Ekers, R. D. & Moffet, A. T., 1968. *Nature*, **220**, 756.
Ekers, R. D. & Moffet, A. T., 1969. *Astrophys. J.*, **158**, L1.
Endean, V. G. & Allen, J. E., 1970. *Nature*, **228**, 348.
Gold, T., 1969. *Nature*, **221**, 25.
Graham, D. A., Lyne, A. G. & Smith, F. G., 1970. *Nature*, **225**, 526.
Graham, D. A., 1971. *Nature*, **229**, 326.
Heiles, C., Campbell, D. B. & Rankin, J. M., 1970. *Nature*, **225**, 526.
Heiles, C. & Rankin, J. M., 1971. *Proc. I.A.U. Symp.*, No. 46, Reidel.
Hunt, G. C., 1971. *Mon. Not. R. astr. Soc.*, **153**, 119.
Komesaroff, M., Morris, D. & Cooke, D. J., 1970. *Astrophys. Lett.*, **5**, 37.
Lyne, A. G. & Rickett, B. J., 1968. *Nature*, **218**, 326.
Lyne, A. G., 1971a. *Proc. I.A.U. Symp.* No. 46, Reidel.
Lyne, A. G., 1971b. *Mon. Not. R. astr. Soc., Short Communications*, **153**, 27P.
Manchester, R. N., 1970. *Nature*, **228**, 264.
Manchester, R. N., 1971. *Proc. I.A.U. Symp.* No. 46. Reidel.
Morris, D., Schwarz, U. J. & Cooke, D. J., 1970. *Astrophys. Lett.*, **5**, 181.
Radhakrishnan, V. & Cooke, D. J., 1969. *Astrophys. Lett.*, **3**, 225.
Schonhardt, R., 1971. *Proc. I.A.U. Symp.* No. 46. Reidel.
Schwarz, U. J. & Morris, D., 1971. *Astrophys. Lett.*, **7**, 185.
Shitov, Yu. P., 1971. *Nature*, **229**, 179.
Smith, F. G., 1968. *Nature*, **220**, 891.
Smith, F. G., 1969. *Nature*, **223**, 934.
Smith, F. G., 1970a. *Mon. Not. R. astr. Soc.*, **149**, 1.
Smith, F. G., 1970b. *Nature*, **228**, 913.
Staelin, D. H. & Reifenstein, E. C., 1969. *Astrophys. J.*, **156**, L121.
Sutton, J. M., Staelin, D. H., Price, R. M. & Weimer, R., 1970. *Astrophys. J.*, **159**, L89.
Taylor, J. H. & Huguenin, G. R., 1969. *Nature*, **221**, 816.
Vitkevich, V. V. & Shitov, Yu. P., 1970a. *Nature*, **225**, 248.
Vitkevich, V. V. & Shitov, Yu. P., 1970b. *Nature*, **226**, 1235.
Wampler, E. J., Scargle, J. D. & Miller, J. S., 1969. *Astrophys. J.*, **157**, L1.
Zeissig, G. A. & Richards, D. W., 1969. *Nature*, **222**, 150.